European Commission

JRC TECHNICAL REPORT

International Spectroradiometer Intercomparison 2023 Final Report

Pavanello, D., Alessandrini, S., Antonelli, A.

2023

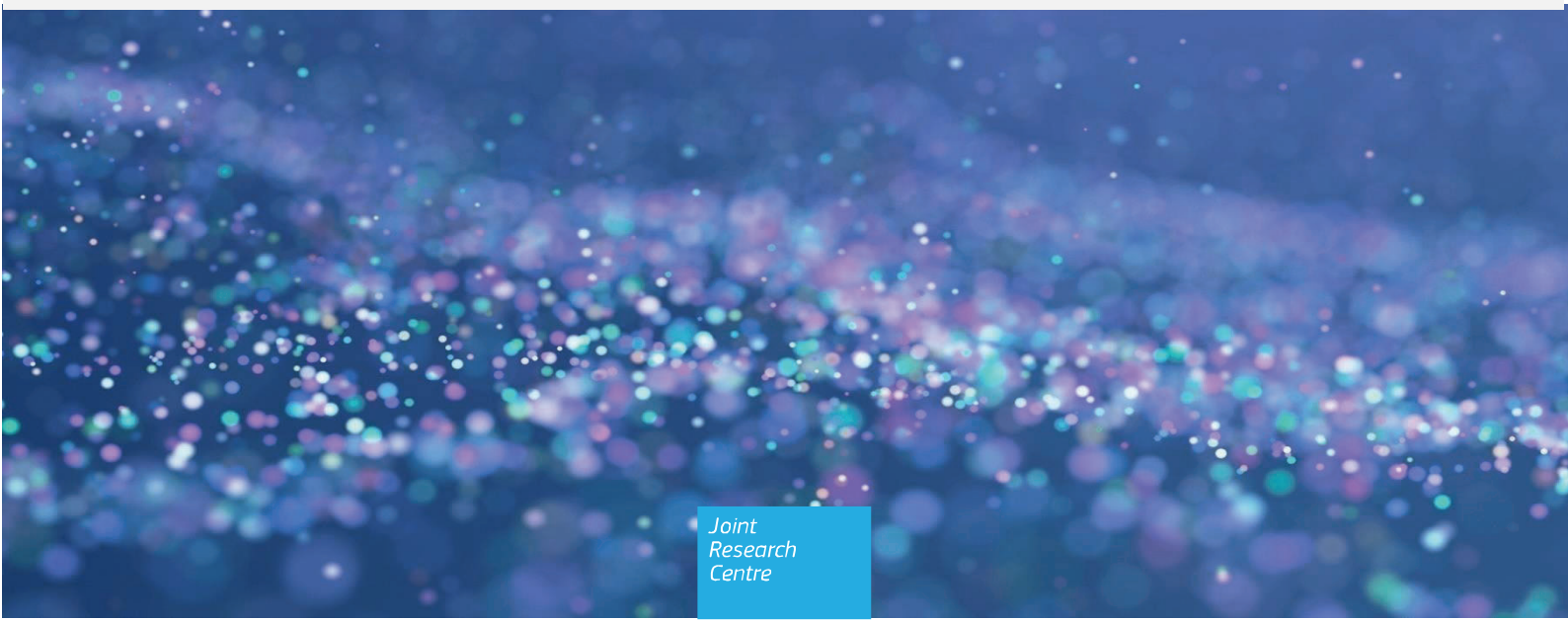

Joint Research Centre

This publication is a Technical report by the Joint Research Centre (JRC), the European Commission's science and knowledge service. It aims to provide evidence-based scientific support to the European policymaking process. The contents of this publication do not necessarily reflect the position or opinion of the European Commission. Neither the European Commission nor any person acting on behalf of the Commission is responsible for the use that might be made of this publication. For information on the methodology and quality underlying the data used in this publication for which the source is neither Eurostat nor other Commission services, users should contact the referenced source. The designations employed and the presentation of material on the maps do not imply the expression of any opinion whatsoever on the part of the European Union concerning the legal status of any country, territory, city or area or of its authorities, or concerning the delimitation of its frontiers or boundaries.

Contact information
Name: Diego Pavanello
Address: European Commission Joint Research Centre, via E. Fermi 2749 Ispra (IT)
Email: diego.pavanello@ec.europa.eu
Tel.:+39 0332 78 6449

EU Science Hub
https://joint-research-centre.ec.europa.eu

JRC136281

Ispra: European Commission, 2023

How to cite this report: Pavanello, D., Alessandrini, S. and Antonelli, A., *International Spectroradiometer Intercomparison 2023 Final Report*, European Commission, Ispra, 2023, JRC136281.

Contents

Abstract

The International Spectroradiometer Intercomparison (ISRC) is a metrological event in the field of solar radiation measurements. The ISRC is managed by the European Solar Test Installation (ESTI) laboratories of the European Commission Joint Research Centre on an annual basis. The eleventh edition was in June 2023 at the Astronomical Observatory of Lignan, Aosta Valley, Italy.

The event consists of a week of uninterrupted measurements of the solar radiation by the instruments of different participants, with the ESTI instrumentation acting as reference for the performance evaluation of spectroradiometers and the calibration of pyranometers and pyrheliometers. In addition, a restricted intercomparison between ten absolute cavity radiometers (ACR) was performed as a dedicated section of the event; in this case the assigned value (reference) has been calculated as the average of the eight cavities with a valid WRR factor from the last IPC in Davos (2021).

Starting in 2011, the first ISRC focused primarily on photovoltaic research and applications. Over the years, the range of interested participants has gradually expanded, encompassing not only laboratories in the PV field, but also space agencies, national metrological institutes (NMI), university and research groups, manufacturers of measurement equipment operating in the fields of climatology and meteorology.

The physical quantities measured during the campaign were the broadband solar irradiance (direct, diffuse and global normal) and the spectrally resolved spectral irradiance (direct and global normal).

The present report summarizes the results of the whole ISRC, divided in four sections: in the first section the calculated sensitivities of the participating pyranometers and pyrheliometers are given; the second section is dedicated to the performance indicators of the spectroradiometers; the third section contains a summary of the Intercomparison restricted to the absolute cavity radiometers; finally, the fourth part contains general information about the prototype instruments present at the Intercomparison.

Prototype instruments were not comparable directly with the reference instruments; their interest in participating at the ISRC was mainly to collect data for further development of the instruments or validation of mathematical models.

Foreword by Christian Thiel

The Joint Research Centre (JRC) is a Directorate-General of the European Commission. Its portfolio is under the responsibility of Iliana Ivanova, Commissioner for Innovation, Research, Culture, Education and Youth. The JRC is present in five different Member States of the EU, with six sites in Brussels and Geel (Belgium), Ispra (Italy), Petten (The Netherlands), Karlsruhe (Germany) and Seville (Spain) with more than 2000 staff.

The JRC activities are grouped in different portfolios, with different scope such as Civil Security, Economy and Finance, Environment, Climate Change, Energy and Transport, Food and Migration.

Within the energy and mobility field, the European Solar Test Installation laboratory (ESTI) is a European reference laboratory for calibration of photovoltaic (PV) devices and for the verification of energy generation. ESTI's unique set of indoor and outdoor facilities allows the measurements of all PV technologies and almost any device size.

To guarantee validity, all measurements (including PV) are required to have an unbroken traceability chain to international primary measurement standards as well as a calculation of their uncertainty. For PV devices the most important and difficult aspect is the irradiance determination, for which ESTI is accredited for three methods. The global sunlight method (1st method) and the direct sunlight method (2nd method) transfer the irradiance calibration from two cavity radiometers, which are calibrated every five years against the World Radiometric Reference at the International Pyrheliometer Comparison held in Davos, Switzerland. The solar simulator method (3rd method) makes reference to the international irradiance scale, as represented by a standard lamp.

ESTI maintains a laboratory management system compliant to the ISO/IEC 17025 and is accredited for the calibration of PV devices (LAT 225) by the Italian accreditation body Accredia.

Since 2011 ESTI manages the International Spectroradiometer Intercomparison (ISRC). Spectroradiometry has become a key discipline in order to achieve precise measurements on any PV device; for this reason, the ISRC began with the participation of actors within the PV community, from top level laboratories to industry and universities. Since the previous edition in June 2022 and also this year other scientific areas have been touched by the ISRC, in particular meteorology and climatology. I thank all JRC colleagues who have organized this year's ISRC, all participants who made it a success and the Astronomical Observatory of the Aosta Valley for allowing us to use their facility for this year's ISRC.

The ISRC is now a key element in the portfolio of the ESTI activities, and I wish for the upcoming years an increase in the number of participants and instruments, to give to the ISRC more and more recognition within the scientific community.

Foreword by Jean-Marc Christille

The Astronomical Observatory of the Autonomous Region of the Aosta Valley (OAVdA) and the Planetarium of Lignan are located in the Saint-Barthélemy Valley, in the Italian Alps along the border area with France and Switzerland, in the small mountain village of Lignan, at almost 1,700 m a.s.l. and 16 km from the town of Nus. The OAVdA and the Planetarium are managed by the non-profit organisation Fondazione Clément Fillietroz-ONLUS, hereafter FCF, whose founder members are the Regional Government of the Autonomous Region of the Aosta Valley, the Unité des Communes valdôtaines Mont-Émilius (formerly Mont-Émilius Mountain Community), and the Town Administration of Nus.

Today, the OAVdA is carrying out six institutional research projects. They concern: the investigation of Solar System bodies (Solar Corona, Asteroids & Fireballs); the monitoring of galaxies (Active Galactic Nuclei); the study of stars in the Milky Way for the search of exoplanets (Extrasolar Planets); the installation and operation at the South Pole, at the Concordia base in Dome C, of the robotic International Telescope Maffei-ITM for infrared observations (Antarctica); the study of the large-scale structure of the cosmos, including the participation in working groups of the ESA's Euclid and LISA space missions (Cosmology).

Over time, our researchers have identified several innovative solutions for the advancement of their studies. This has led to the formation of a specific technological expertise that has enabled the FCF to engage, since 2011, in the field of technology transfer, even in areas of potential industrial and commercial interest: from smart agriculture to cultural heritage monitoring, from climate monitoring to machine learning and computational genomics. Including completed and ongoing projects, the OAVdA has so far been involved in fifteen major scientific research and technology transfer projects, either as a partner or lead partner.

In addition, our researchers personally design and conduct educational and outreach activities for schools and the public. We strongly believe that there is an inseparable link between scientific research, education and outreach: in fact, it is scientific research who produces the original contents and knowledge to be communicated through educational and outreach activities. In twenty years our centre has recorded some 200,000 admissions among students and the general public, with an additional admittance of 100,000 when we consider the participation in events taking place away from Saint-Barthélemy, such as lessons in the schools, lectures for several science festivals and so on.

The Lignan area received - first in Italy and fourth in the world at the time - the prestigious international Starlight Stellar Park certification for the quality of the night sky and the protection against the light pollution. This certification is recognized by the United Nations Educational, Scientific and Cultural Organization (UNESCO), the World Tourism Organization (UNWTO) and the International Astronomical Union (IAU).The Fondazione Clément Fillietroz-ONLUS, with the facilities of the OAVdA and the Planetarium, thus represents the main institution in the Aosta Valley for basic research, the development of related technologies, and the communication of astronomy and astrophysics to the general public and students. Thanks to the skills and commitment of its staff, the FCF has organised more than 40 summer schools, winter schools, hackathons and scientific meetings at both national and international level. We have been very happy to host the 2022 and 2023 International Spectroradiometer and Broadband Radiometer Intercomparison campaigns, hoping that it could become a scheduled event in the next years, attracting researchers worldwide and letting them exploit the great potentiality of the Saint-Barthélemy Valley and the whole Aosta Valley region as a very unique open-air natural laboratory.

Acknowledgements

The authors would like to warmly acknowledge all the staff of the Astronomical Observatory of the Aosta Valley (OAVDA) in Lignan, for the great collaboration before and throughout the event. In particular, we would like to mention the Director Jean-Marc Christille, the scientist Paolo Calcidese and the responsible for communication Andrea Bernagozzi.

We would like also to acknowledge the precious help of Willem Zaaiman, former JRC official, in the data analysis process of the pyranometers and pyrheliometers.

Finally, we thank the contribution of our JRC colleagues Harald Müllejans and Nigel Taylor for the review of the manuscript.

Authors

Diego Pavanello

Adriano Antonelli

Stefano Alessandrini

1 Introduction

The International Spectroradiometer Intercomparison (ISRC) has reached its 11th edition this year, hosted for the second time by the Astronomical Observatory of the Aosta Valley (OAVdA).

The ISRC started in 2011 at the ENEA site of Portici (NA), in Italy, with the aim to assess the comparability of different measurement chains for the solar spectral irradiance between the participating institutions [1]. As an accredited reference laboratory in the field of photovoltaics, ESTI's main interest is related to metrological aspects of the performance of different PV technologies [2]. While crystalline silicon devices, with all their different flavors available nowadays on the market, can be considered as well known technologies with respect to their dependency on spectral irradiance, this is not yet true for new materials like perovskites (single and tandem), dye-sensityzed and organic [3-7]. Considering this aspect, a precise characterization of the incoming light spectrum has become a crucial metrological factor to reduce (or at least better characterize) the measurement uncertainties for these devices.

A second aspect concerns the measurement of the direct normal (DNI or beam) and global normal (GNI) incident solar radiation using so-called broadband sensors, in particular pyranometers and pyrheliometers [8-10]. A precise calibration of such instruments, performed using absolute cavity radiometers (ACR) as reference, is a key factor for all the applications involving solar radiation: to have reliable outdoor performance estimations of PV systems, to improve mathematical models related to meteorology and climatology, to perform secondary calibrations of other instruments at factory level, to monitor the energy production of PV installations.

The aforementioned aspects are key elements for the successful achievement of the ambitious goals set be the European Green Deal. The EU has adopted several actions to promote climate action for the protection of the environment, achieve energy transition and create a circular economy of products. The renewable energy with the largest scope in terms of scientific development, innovation, industrial transfer and impact is solar photovoltaic energy. The ISRC acts in the framework of the JRC activities for the development of international standards, research for the metrology used to measure the photovoltaic performance and estimation, in particular for innovative technologies, providing independent reference data for EU research laboratories and industry.

The present report presents the results of the 11th ISRC, planned from 26-30 June 2023, but effectively held only from 26-28 June due to adverse weather conditions. Due to the reduced duration, the sensitivity factors calculated for the pyranometers and pyrheliometers are not compliant to the requirements of ISO 9059 and ISO 9846. Also the intercomparison restricted to the cavity radiometers has been impacted, having only two usable days of measurements. The assessment of the spectroradiometers have been less impacted, with a sufficient number of stable spectral data extracted among the almost 24000 spectra acquired and analyzed.

2 Participating institutions

The following table summarizes (in alphabetical order) the list of participating institutions, their role and participation sectors, and contact websites.

Table 1: Participating Institutions

JRC / ESTI		Organizer of the ISRC. Reference for pyranometers, pyrheliometers and spectroradiometers. Intercomparison of ACR.	JRC: https://joint-research-centre.ec.europa.eu/index_en ESTI: https://joint-research-centre.ec.europa.eu/european-solar-test-installation_en
CIEMAT		Intercomparison of ACR	https://www.ciemat.es/
DAVOS INSTRUMENTS AG		Intercomparison of ACR	https://www.davos-instruments.ch/
Directorate General of Meteorology Morocco		Broadband sensors	https://www.marocmeteo.ma/
ENEA (Portici)		Spectroradiometers Intercomparison Broadband sensors	https://www.portici.enea.it/
ESA ESTEC European Space Agency		Spectroradiometers Intercomparison	ESA: https://www.esa.int/
EURAC		Spectroradiometers Intercomparison Broadband sensors	https://www.eurac.edu
IEP – Instituto Eletrotecnico Portugues		Broadband sensors	https://www.iep.pt
Officina del Sole		Broadband sensors	http://www.o-sole.it
PV Lab		Spectroradiometers Intercomparison	https://www.pv-lab.de
RSE – Ricerca Sistema Energetico		Spectroradiometers Intercomparison Broadband sensors	https://www.rse-web.it
SERIS		Spectroradiometers Intercomparison Broadband sensors	https://www.seris.nus.edu.sg
SUPSI		Spectroradiometers Intercomparison Broadband sensors	https://www.supsi.ch
University of Milan-Bicocca		Prototype of bolometers system	https://www.fisica.unimib.it
Dr. Willem Zaaiman Former JRC researcher		Broadband sensors Intercomparison of ACR	
Kevin Murray Former North West Regional College		Spectroradiometers Intercomparison Broadband sensors	

3 Pyranometers and pyrheliometers

This section presents the results of the analysis of the sensitivity coefficients for the participating pyranometers and pyrheliometers. The pyranometers were all mounted on a large area tracker (2m x 2m size), while the pyrheliometers were on a second smaller tracker. The reference absolute cavity radiometers (ACR) and the reference pyranometer measuring the diffuse irradiance were on a third tracker; to measure the diffuse component of the irradiance the pyranometer was always kept shaded by a shading disc. The alignment of all the trackers was checked periodically every 10-15 minutes throughout all the days[1]. The acquisition timing was ruled by the ACR system.

3.1 Instruments

Table 2: list of pyranometers and pyrheliometers

Pyranometers	**Pyrheliometers**
Hukseflux SR20_2026	Eppley NIP_37893E6
Hukseflux SR20_3746	Eppley NIP 37886E6
Kipp&Zonen CMP10_191709	Eppley NIP_22029E6
Kipp&Zonen CMP11_070362	Eppley NIP_25668E6
Kipp&Zonen CMP11_090904	Eppley NIP_27092E6
Kipp&Zonen CMP11_090905	Eppley NIP_27818E6
Kipp&Zonen CMP11_114178	Eppley NIP_34854E6
Kipp&Zonen CMP11_152486	Kipp&Zonen CHP1_110545
Kipp&Zonen CMP21_100410	Kipp&Zonen CHP1_110709
Kipp&Zonen CMP21_120923	Kipp&Zonen CHP1_120985
Kipp&Zonen CMP21_133060	Kipp&Zonen CHP1_131099
LSI_LASTEM	Kipp&Zonen CHP1_150317
EKO MS80_S19046225	Hukseflux DR01_10_8123
EKO MS80_S22008376	Hukseflux DR01_8058
EKO MS802_F02028F	Hukseflux DR01_8174
EKO MS802_F02030F	Hukseflux DR01_8317
EKO MS802_F02031F	EKO MS57_S110418
EKO MS802_F10165F	EKO MS57_S1906713
Eppley PSP_25838F3	
Eppley PSP_34832F3	
Kipp&Zonen CMP11_115395	
Kipp&Zonen CMP21_100453	
Kipp&Zonen CM22_0300076	
Kipp&Zonen SMP21_220272	

[1] The nominal accuracy of the used trackers is <0.01°.

3.2 Data acquisition and evaluation

The signals of the absolute cavity radiometers, calibrated pyrheliometers and a shaded CM22 pyranometer were simultaneously acquired by an in-house software developed at ESTI. All the reference instruments were connected to data loggers HP 34970A. The control and data acquisition systems of the reference instruments were independent from the systems connected to the broadband instruments of the participants.

The participants' pyranometers and pyrheliometers were connected to two data loggers HP34970A, connected via GPIB cable to a unique computer, which sent the trigger signals to both the systems for a synced data acquisition.

The time sync between the different systems was performed every morning before starting the acquisitions, using a GPS signal, and setting all the clocks at GMT+1. It is worth noting that in Italy the Local Time was GMT+2 in June, but the solar time GMT+1.

The timing of the ESTI's PMO6 cavities was set to cycles of 45 seconds with shutter closed alternated to 45 seconds with shutter opened. At the end of each cycle a single data point was acquired. The four calibrated pyrheliometers and diffuse pyranometer acquired a valid irradiance point every 45 seconds as well, thus including the periods where the ACR had the shutter closed. A more dense temporal resolution allowed to improve the sky stability control for the data post-processing. The instruments of the participants were acquired every 45 seconds synchronously with the cavities.

Data were filtered according to the criteria listed in 3.3 in order to consider for the evaluation only those points acquired in stable sky conditions. Due to the weather conditions during the days of the intercomparison, for none of the instruments the minimum number of three acceptable days (with a sufficient number of points in clear sky conditions) was achieved.

The sensitivity value of each instrument was then calculated as the arithmetic average of the entire time series covering all the days, including the so-called "daily variation" and expanded standard deviation in the uncertainty budget. Each point of the time series is the measured voltage value of the specific instrument linearly corrected to 1000 W/m^2 considering the corresponding reference irradiance value (either DNI or GNI depending on the instrument type). Therefore the final expanded uncertainty value is specifically calculated for each instrument, and given assuming a normal distribution with coverage factor k = 2 (about 95% probability).

3.3 Data filtering

Data were acquired during the entire day independently on the sky stability, which was assessed afterwards during the data post-processing. The entire raw data set of the ISRC has been given to all the participants. From the raw data set, only the points fulfilling the criteria for a suitable sky stability have been kept for data analysis, whilst all the others have been removed.

The filtering criteria are summarized as follows:

- DNI(t) ≤ 1000 W/m^2
- DNI(t) ≥ 700 W/m^2
- GNI(t) ≤ 1100 W/m^2
- Diffuse (t) ≤ 300 W/m^2
- Maximum difference between the two ESTI's reference ACRs: less than 2 W/m^2
- Maximum DNI difference in a period of 90 seconds (measured by the reference pyrheliometers): 3 W/m^2
- Maximum ratio between any reference pyrheliometer and the ACR average: $0.998 \leq R_k \leq 1.002$

A second layer of filtering is the performed individually for each instrument's data series to flag suspicious points affected by artefacts. Flagged points are then singularly evaluated and eventually manually removed from the series.

In order to give a course idea of the impact of data filtering on the total amount of acquired points, on the days used for the calculations, about 85% of the raw data have been filtered out.

3.4 Responsivity factors

Due to the adverse meteorological conditions in the Aosta Valley during the days of the Intercomparison, for all the instruments only two days have been deemed as acceptable for the calculation of their sensitivity factors. On these days quasi-clear sky conditions were achieved on intervals long enough to measure a sufficient number of data series. However, none of the coefficients shown in this section is compliant to the requirements of the ISO 9846 (for pyranometers) and ISO 9059 (for pyrheliometers) and therefore they shall be considered as indicative only.

Table 3: sensitivity factors and associated uncertainties of pyranometers and pyrheliometers

	CF $\mu V/(Wm^{-2})$	UC (k=2) $\mu V/(Wm^{-2})$	UC(k=2) (%)	Comment (see explanations)
SR20_2026				Too large difference between days
SR20_3746				Too large difference between days
CMP10_191709	9.07	0.09	1.03%	
CMP11_070362	8.72	0.08	0.95%	
CMP11_090904	9.06	0.07	0.81%	
CMP11_090905	8.84	0.07	0.77%	
CMP11_114178	8.85	0.07	0.82%	
CMP11_152486	9.10	0.08	0.91%	
CMP21_100410	9.05	0.07	0.75%	
CMP21_120923				Too large difference between days
CMP21_133060	8.97	0.07	0.81%	
LSI_LASTEM	30.26	0.44	1.45%	
MS80_S19046225				Too large difference between days
MS80_S22008376	8.97	0.12	1.32%	Only one day considered
MS802_F02028F				Too large difference between days
MS802_F02030F				Too large difference between days
MS802_F02031F				Too large difference between days
MS802_F10165F	6.94	0.07	0.94%	
PSP_25838F3	8.81	0.12	1.35%	Only one day considered
PSP_34832F3				Too large difference between days
CMP11_115395	9.04	0.11	1.18%	Only one day of measurements
CMP21_100453	9.00	0.11	1.21%	Only one day of measurements
CM22_0300076	9.40	0.11	1.13%	Only one day of measurements
NIP_37893E6				Too large difference between days
NIP37886E6				Too large difference between days
NIP_22029E6	7.81	0.09	1.19%	
NIP_25668E6	7.46	0.06	0.82%	
NIP_27092E6	8.83	0.07	0.84%	
NIP_27818E6	8.28	0.08	0.93%	
NIP_34854E6	7.57	0.05	0.72%	

CHP1_110545	7.68	0.08	1.07%	Only one day of measurements
CHP1_110709	7.92	0.04	0.52%	
CHP1_120985	7.79	0.04	0.57%	
CHP1_131099	8.27	0.04	0.52%	
CHP1_150317	7.71	0.06	0.78%	Only one day of measurements
DR01_10_8123				Too large difference between days
DR01_8058	8.56	0.04	0.52%	
DR01_8174	10.26	0.05	0.48%	
DR01_8317	11.31	0.07	0.61%	
MS57_S110418	7.07	0.17	2.39%	Only one day of measurements
MS57_S1906713	7.22	0.12	1.70%	

Explanation of the comments

No comment: the indicated sensitivity factor and corresponding expanded uncertainty can be given (as indicative and without certificate). In this case data were sufficient to calculate a stable value during either one or two days. The given values and corresponding uncertainties have been calculated using a primary calibration method and then checked against a secondary analysis method with coherent results.

Too large difference between days: data were present for two days, however the daily values of the sensitivity coefficients were incoherent between themselves. Value not given.

Only one day considered: the given sensitivity value has been calculated basing on a single day of measurements; the data series was sufficiently good to indicate an estimate. The given value has been checked against a secondary method analysis and was consistent with it. The measurement uncertainty for the given value has been increased to compensate the absence of the daily variation component.

Absence of value: the data series was not sufficient to indicate any reasonable value.

4 Spectroradiometers

This section presents the results of the analysis of the spectroradiometers measured at the ISRC. The instruments of the participants were all mounted on a large MEMS tracker, while the EKO Wiser system (MS701-MS710-MS712) serving as reference for Direct Normal Spectral Irradiance and the CAS140+CAS140CTS system serving as reference for Global Normal Spectral Irradiance were mounted on two different trackers. The alignment of all of them was checked periodically every 10-15 minutes throughout all the campaign.

The timing was agreed between all the participants having a data acquisition software allowing automatic acquisitions, and was set to one spectrum every minute. Participants having to do manual acquisitions acquired less spectra, but nevertheless all the clocks were synchronized with the reference clock. The spectra were acquired at the beginning of each minute (hh:mm:00). The list of the spectroradiometers is presented in the following table.

Table 4: List of spectroradiometers.

	Manufacturer	Model and s/n	Owner	Comment
GNI	Instrument Systems	CAS140CT + CAS140CTS	JRC – ESTI	Reference for GNI
	Avantes	AvaSpec	ENEA	
	Ocean Optics	RaySphere 900	ESA	
	Instrument Systems	CAS140	PVLAB	
	Avantes	Avaspec	SERIS	
	Avantes	AvaSpec	SUPSI	
	EKO	MS710 + MS712	SUPSI	
	EKO	MS700	K. Murray	
DNI	EKO	MS701 + MS710 + MS712	JRC – ESTI	Reference for DNI
	Spectrafy	SolarSIM D2	RSE	Hybrid instrument (*)
	Spectrafy	SolarSIM D2	JRC – ESTI	Hybrid instrument (*)

(*): the instrument uses a numerical model to calculate the DNI solar spectrum based on the short circuit current measurements of six filtered photodiodes.

The two reference systems are internally calibrated at ESTI on an annual basis, and additionally before and after any external measurement campaign. The spectroradiometer calibration is ISO/IEC 17025 accredited. They are traceable to both NPL and PTB via calibrated standard lamps.

4.1 Data filtering and evaluation

Only a limited number of spectra have been considered for evaluation among the almost 24000 spectra measured during the campaign. The time frames selected to analyse the performance of spectroradiometers are distributed among three days and encompass 7.5 hours of continuous measurements.

Within the stable time frames, for both DNI and GNI spectral irradiance, a reference spectrum has been acquired at times t_k, synchronously with all the other participants. The sync signal was given by a dedicated GPS and checked periodically by everybody against the clock of the references.

The timing of all the spectroradiometers was set at one sample per minute; however, several instruments were set to measure on a different time base, varying from one sample every 10 seconds to one sample every 5 minutes. A script automatically scanned the whole spectra data set in order to build “spectra sets”. All the spectra measured at $t_k \pm 5$ seconds have been grouped to

form a set $S(t_k)$ of spectra for the instant t_k . Each set $S(t_k)$ contains as first element the reference spectrum, but not necessarily all the participants samples. Another program then divided the sets per participant.

The following functions have been considered of interest for the intercomparison:

- $R_{10}(\lambda_1, \lambda_2)$: absolute spectral content in narrow spectral bands (10 nm width) within the spectral limits imposed by each instrument model
- $R_{10}^*(\lambda_1, \lambda_2)$: relative spectral content respect to the entire integral of the same spectrum with the limits of the previous point

The former contains all the elements of the traceability chain of each participant and the reference as well, while the latter is a "shape-factor" not sensitive to constant errors independent of the wavelengths.

The two following narrowband quantities are expressed by:

$$R_{10}(\lambda_1, \lambda_2) = \frac{\int_{\lambda_1}^{\lambda_2} E_i(\lambda) d\lambda}{\int_{\lambda_1}^{\lambda_2} E_{REF}(\lambda) d\lambda} \qquad \text{(Eq. 1)}$$

and

$$R_{10}^*(\lambda_1, \lambda_2) = \frac{\dfrac{\int_{\lambda_1}^{\lambda_2} E_i(\lambda) d\lambda}{\int_{\lambda_{min}}^{\lambda_{max}} E_i(\lambda) d\lambda}}{\dfrac{\int_{\lambda_1}^{\lambda_2} E_{REF}(\lambda) d\lambda}{\int_{\lambda_{min}}^{\lambda_{max}} E_{REF}(\lambda) d\lambda}} \qquad \text{(Eq. 2)}$$

In the following plots the error bars refer to the expanded standard deviation of each measured data series, obtained by multiplying the standard deviation by the coverage factor k = 2 (assuming a normal distribution). Each series (let's say series number q) consists of the number of sets including the participant's spectrum and the corresponding reference spectrum. Both have then been linearly interpolated on an evenly spaced grid of 0.1 nm. A linear interpolation is sufficient because all the spectroradiometers have a sufficiently good wavelength resolution (although the uncertainty of the wavelength alignment is usually higher than the resolution and not constant in the entire range). It is worth considering that the interpolation process solves the issue that all the spectroradiometers have different wavelength axis, and that they are usually unevenly spaced.

The two spectra belonging to the q^{th}-set (reference and participant acquired at the same time) have then divided in bands with 10 nm width and the partial integrals calculated to obtain the two parameters $R_{10,q}(\lambda_1, \lambda_2)$ and $R_{10,q}^*(\lambda_1, \lambda_2)$. For each spectral band all the couples of spectra acquired in the same series have been used to calculate the average and standard deviation for each spectral band.

4.2 The intermediate file format .isrc

To all the participants to the ISRC was given the possibility to submit their measured spectra in their preferred file format. Thus the raw data set was initially composed by files containing one

spectrum, files containing many spectra by columns or by rows, files with structured and non-structured filenames and so on.

The first step in the data analysis process was the conversion of all the different formats into a unique file type, conceived on purpose for the Intercomparison, with the extension .isrc.

The filename is structured as follows:

[ID]_[YYYY]_[MM]_[DD]_[hh]_[mm]_[ss]_[sfm].isrc

with

ID:	string identifying the participant and instrument
YYYY:	year (four characters)
MM:	month (two characters)
DD:	day (two characters)
hh:	hour (two characters)
mm:	minute (two characters)
ss:	second (two characters)
sfm:	seconds from midnight

The seconds from midnight are calculated as

$$sfm = 3600hh + 60mm + ss \quad \text{(Eq. 3)}$$

and the time is referred to GMT+1. Seconds from midnight have been added in the filename to be able at a later stage to find the closest spectra without opening the files, thus reducing the computational time. The file is structured in two columns tab separated, containing the wavelength axis (in nm) and the measured spectrum (in W/(m^2 nm)). No data manipulation such as wavelength range cut or interpolation is done at this stage yet.

4.3 Temporal syncing

After the conversion of all the spectra to the format .isrc the temporal alignment has been checked. The synchronization of all the spectra with the reference data series is essential to build the sets by finding, for each reference spectrum, the closest one of each participant. Although the time frames considered for the analysis included only spectra acquired in clear sky conditions, the maximum allowed distance to couple two spectra was set to 5 seconds. The clocks of all the data acquisition systems were synced every morning using a dedicated GPS signal, although the precision of the operator might lead to a misalignment of a few seconds.

In order to perform the alignment, for each spectrum of each participant the integrated irradiance between 400 – 1000 nm has been calculated, being this reduced range common to all the instruments. During the day, the irradiance drops due to passing clouds have been detected and the participant's time axis have been shifted if not properly aligned.

4.4 Global Normal Spectral Irradiance

4.4.1 ENEA Avantes Avaspec

Absolute Ratio R_{10}

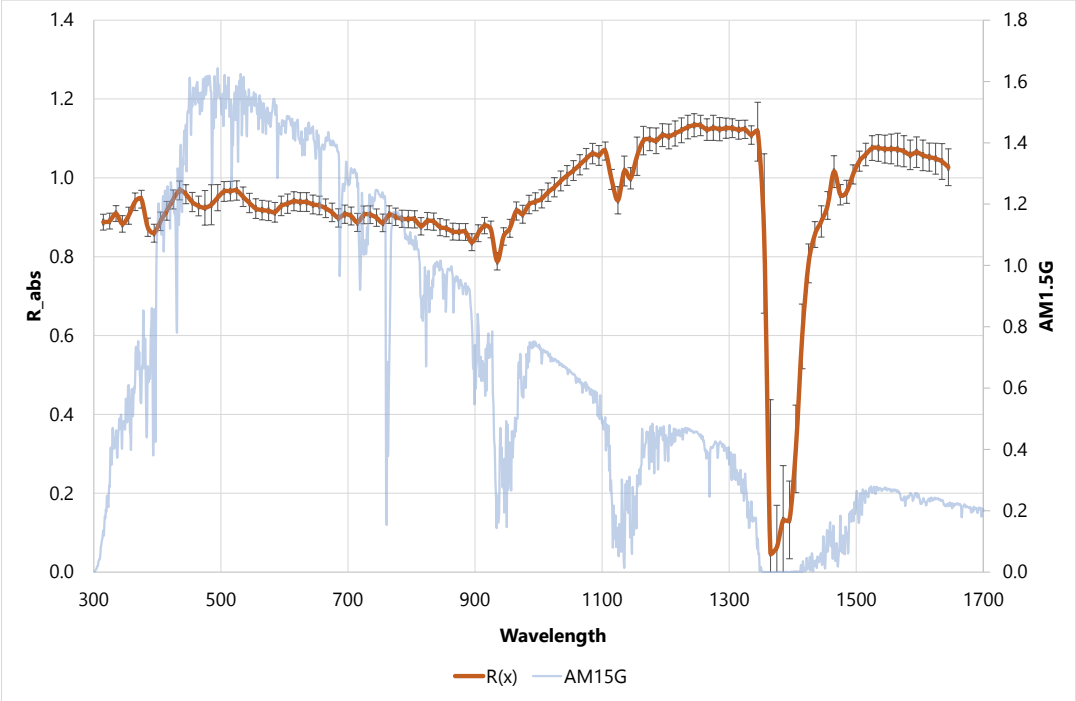

Relative Ratio R^*_{10}

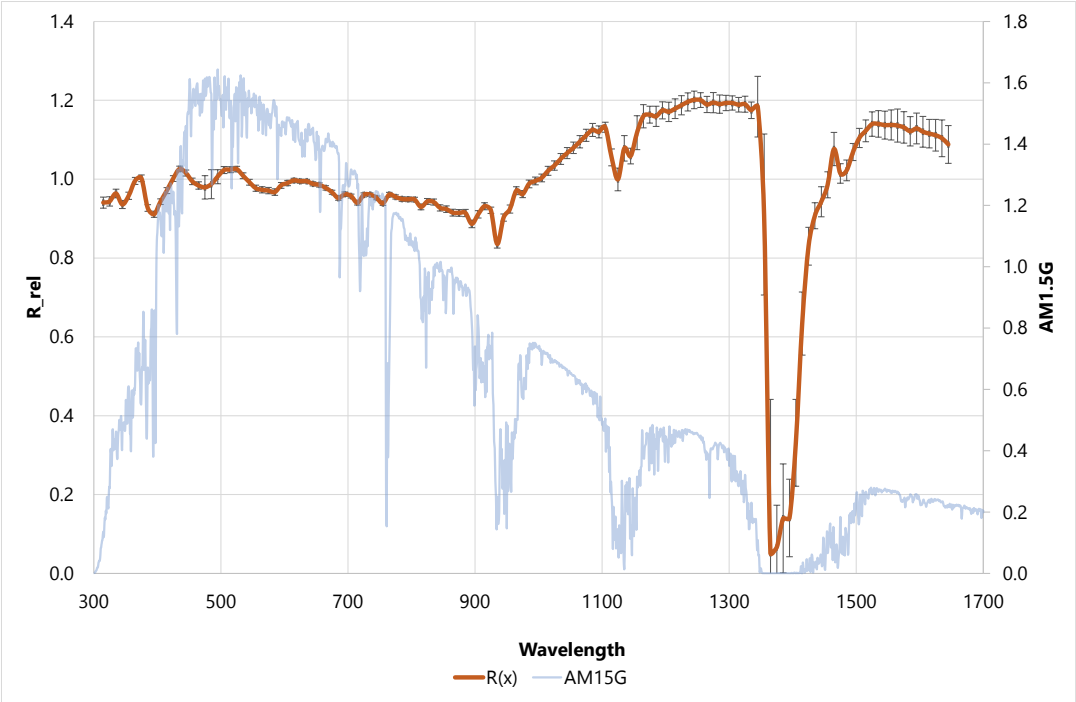

Figure 1 Performance indicators of spectroradiometer Avantes Avaspec (ENEA)

Table 5: tabulated values of performance indicators Avantes Avaspec (ENEA)

λ	R10 absolute	R10 relative	λ	R10 absolute	R10 relative
310 - 320 nm	0.8875 ± 0.0177	0.9405 ± 0.0131	**980 - 990 nm**	0.9323 ± 0.0219	0.9880 ± 0.0096
320 - 330 nm	0.8904 ± 0.0179	0.9436 ± 0.0112	**990 - 1000 nm**	0.9393 ± 0.0214	0.9954 ± 0.0097
330 - 340 nm	0.9093 ± 0.0183	0.9636 ± 0.0106	**1000 - 1010 nm**	0.9467 ± 0.0219	1.0032 ± 0.0098
340 - 350 nm	0.8832 ± 0.0184	0.9359 ± 0.0097	**1010 - 1020 nm**	0.9636 ± 0.0227	1.0211 ± 0.0115
350 - 360 nm	0.9039 ± 0.0196	0.9579 ± 0.0088	**1020 - 1030 nm**	0.9761 ± 0.0236	1.0344 ± 0.0122
360 - 370 nm	0.9395 ± 0.0210	0.9956 ± 0.0090	**1030 - 1040 nm**	0.9922 ± 0.0248	1.0514 ± 0.0146
370 - 380 nm	0.9458 ± 0.0213	1.0023 ± 0.0085	**1040 - 1050 nm**	1.0061 ± 0.0254	1.0662 ± 0.0150
380 - 390 nm	0.8746 ± 0.0202	0.9268 ± 0.0079	**1050 - 1060 nm**	1.0186 ± 0.0257	1.0794 ± 0.0156
390 - 400 nm	0.8597 ± 0.0196	0.9110 ± 0.0070	**1060 - 1070 nm**	1.0333 ± 0.0264	1.0950 ± 0.0171
400 - 410 nm	0.8898 ± 0.0209	0.9429 ± 0.0066	**1070 - 1080 nm**	1.0485 ± 0.0272	1.1111 ± 0.0171
410 - 420 nm	0.9162 ± 0.0219	0.9709 ± 0.0074	**1080 - 1090 nm**	1.0615 ± 0.0276	1.1249 ± 0.0184
420 - 430 nm	0.9450 ± 0.0228	1.0014 ± 0.0074	**1090 - 1100 nm**	1.0567 ± 0.0266	1.1198 ± 0.0169
430 - 440 nm	0.9681 ± 0.0231	1.0259 ± 0.0071	**1100 - 1110 nm**	1.0680 ± 0.0244	1.1318 ± 0.0144
440 - 450 nm	0.9585 ± 0.0233	1.0157 ± 0.0078	**1110 - 1120 nm**	0.9958 ± 0.0252	1.0553 ± 0.0225
450 - 460 nm	0.9386 ± 0.0229	0.9946 ± 0.0082	**1120 - 1130 nm**	0.9431 ± 0.0328	0.9994 ± 0.0288
460 - 470 nm	0.9285 ± 0.0232	0.9839 ± 0.0091	**1130 - 1140 nm**	1.0174 ± 0.0387	1.0781 ± 0.0348
470 - 480 nm	0.9240 ± 0.0405	0.9791 ± 0.0290	**1140 - 1150 nm**	0.9988 ± 0.0269	1.0585 ± 0.0209
480 - 490 nm	0.9317 ± 0.0473	0.9873 ± 0.0364	**1150 - 1160 nm**	1.0548 ± 0.0511	1.1177 ± 0.0480
490 - 500 nm	0.9497 ± 0.0316	1.0064 ± 0.0180	**1160 - 1170 nm**	1.0943 ± 0.0396	1.1596 ± 0.0342
500 - 510 nm	0.9655 ± 0.0244	1.0231 ± 0.0091	**1170 - 1180 nm**	1.0980 ± 0.0319	1.1636 ± 0.0249
510 - 520 nm	0.9664 ± 0.0239	1.0240 ± 0.0078	**1180 - 1190 nm**	1.0940 ± 0.0358	1.1593 ± 0.0298
520 - 530 nm	0.9679 ± 0.0238	1.0257 ± 0.0072	**1190 - 1200 nm**	1.1083 ± 0.0321	1.1745 ± 0.0254
530 - 540 nm	0.9520 ± 0.0235	1.0088 ± 0.0073	**1200 - 1210 nm**	1.1049 ± 0.0349	1.1709 ± 0.0287
540 - 550 nm	0.9363 ± 0.0230	0.9922 ± 0.0071	**1210 - 1220 nm**	1.1124 ± 0.0356	1.1788 ± 0.0296
550 - 560 nm	0.9220 ± 0.0229	0.9770 ± 0.0075	**1220 - 1230 nm**	1.1206 ± 0.0351	1.1875 ± 0.0290
560 - 570 nm	0.9181 ± 0.0227	0.9729 ± 0.0077	**1230 - 1240 nm**	1.1287 ± 0.0338	1.1961 ± 0.0275
570 - 580 nm	0.9164 ± 0.0228	0.9710 ± 0.0080	**1240 - 1250 nm**	1.1335 ± 0.0331	1.2012 ± 0.0267
580 - 590 nm	0.9127 ± 0.0227	0.9671 ± 0.0080	**1250 - 1260 nm**	1.1329 ± 0.0294	1.2006 ± 0.0224
590 - 600 nm	0.9289 ± 0.0228	0.9843 ± 0.0072	**1260 - 1270 nm**	1.1224 ± 0.0309	1.1893 ± 0.0243
600 - 610 nm	0.9344 ± 0.0227	0.9902 ± 0.0066	**1270 - 1280 nm**	1.1269 ± 0.0358	1.1941 ± 0.0305
610 - 620 nm	0.9406 ± 0.0227	0.9967 ± 0.0056	**1280 - 1290 nm**	1.1234 ± 0.0332	1.1905 ± 0.0276
620 - 630 nm	0.9387 ± 0.0225	0.9947 ± 0.0051	**1290 - 1300 nm**	1.1259 ± 0.0290	1.1931 ± 0.0232
630 - 640 nm	0.9387 ± 0.0223	0.9947 ± 0.0047	**1300 - 1310 nm**	1.1259 ± 0.0269	1.1931 ± 0.0216
640 - 650 nm	0.9324 ± 0.0221	0.9881 ± 0.0050	**1310 - 1320 nm**	1.1218 ± 0.0268	1.1888 ± 0.0222
650 - 660 nm	0.9299 ± 0.0220	0.9854 ± 0.0053	**1320 - 1330 nm**	1.1231 ± 0.0261	1.1902 ± 0.0242
660 - 670 nm	0.9228 ± 0.0217	0.9779 ± 0.0053	**1330 - 1340 nm**	1.1085 ± 0.0261	1.1747 ± 0.0244
670 - 680 nm	0.9123 ± 0.0214	0.9668 ± 0.0051	**1340 - 1350 nm**	1.1171 ± 0.0834	1.1839 ± 0.0911
680 - 690 nm	0.8983 ± 0.0210	0.9519 ± 0.0052	**1350 - 1360 nm**	0.8588 ± 0.1735	0.9104 ± 0.1859
690 - 700 nm	0.9077 ± 0.0212	0.9619 ± 0.0052	**1360 - 1370 nm**	0.0485 ± 0.0188	0.0515 ± 0.0201
700 - 710 nm	0.9032 ± 0.0207	0.9571 ± 0.0047	**1370 - 1380 nm**	0.0622 ± 0.0067	0.0661 ± 0.0071
710 - 720 nm	0.8870 ± 0.0204	0.9400 ± 0.0051	**1380 - 1390 nm**	0.1315 ± 0.0182	0.1395 ± 0.0193
720 - 730 nm	0.9062 ± 0.0206	0.9602 ± 0.0049	**1390 - 1400 nm**	0.1325 ± 0.0130	0.1406 ± 0.0138

730 – 740 nm	0.9066 ± 0.0205	0.9607 ± 0.0043	**1400 – 1410 nm**	0.3124 ± 0.0347	0.3313 ± 0.0365
740 – 750 nm	0.8989 ± 0.0199	0.9525 ± 0.0043	**1410 – 1420 nm**	0.5979 ± 0.0490	0.6338 ± 0.0508
750 – 760 nm	0.8857 ± 0.0198	0.9385 ± 0.0047	**1420 – 1430 nm**	0.7831 ± 0.0386	0.8299 ± 0.0396
760 – 770 nm	0.9067 ± 0.0203	0.9608 ± 0.0057	**1430 – 1440 nm**	0.8561 ± 0.0282	0.9074 ± 0.0299
770 – 780 nm	0.9010 ± 0.0199	0.9548 ± 0.0052	**1440 – 1450 nm**	0.8896 ± 0.0353	0.9427 ± 0.0360
780 – 790 nm	0.8960 ± 0.0197	0.9495 ± 0.0056	**1450 – 1460 nm**	0.9299 ± 0.0327	0.9855 ± 0.0325
790 – 800 nm	0.8955 ± 0.0197	0.9489 ± 0.0055	**1460 – 1470 nm**	1.0157 ± 0.0409	1.0765 ± 0.0454
800 – 810 nm	0.8948 ± 0.0197	0.9482 ± 0.0056	**1470 – 1480 nm**	0.9572 ± 0.0248	1.0144 ± 0.0251
810 – 820 nm	0.8771 ± 0.0194	0.9295 ± 0.0068	**1480 – 1490 nm**	0.9646 ± 0.0281	1.0222 ± 0.0269
820 – 830 nm	0.8903 ± 0.0193	0.9434 ± 0.0069	**1490 – 1500 nm**	1.0086 ± 0.0243	1.0689 ± 0.0233
830 – 840 nm	0.8890 ± 0.0193	0.9420 ± 0.0072	**1500 – 1510 nm**	1.0424 ± 0.0265	1.1047 ± 0.0268
840 – 850 nm	0.8750 ± 0.0190	0.9272 ± 0.0073	**1510 – 1520 nm**	1.0593 ± 0.0302	1.1226 ± 0.0310
850 – 860 nm	0.8719 ± 0.0186	0.9239 ± 0.0077	**1520 – 1530 nm**	1.0755 ± 0.0336	1.1397 ± 0.0352
860 – 870 nm	0.8636 ± 0.0185	0.9151 ± 0.0078	**1530 – 1540 nm**	1.0758 ± 0.0365	1.1401 ± 0.0383
870 – 880 nm	0.8628 ± 0.0183	0.9143 ± 0.0079	**1540 – 1550 nm**	1.0728 ± 0.0382	1.1369 ± 0.0404
880 – 890 nm	0.8628 ± 0.0184	0.9143 ± 0.0084	**1550 – 1560 nm**	1.0734 ± 0.0406	1.1375 ± 0.0431
890 – 900 nm	0.8366 ± 0.0179	0.8866 ± 0.0084	**1560 – 1570 nm**	1.0719 ± 0.0444	1.1359 ± 0.0476
900 – 910 nm	0.8594 ± 0.0185	0.9107 ± 0.0086	**1570 – 1580 nm**	1.0675 ± 0.0422	1.1313 ± 0.0451
910 – 920 nm	0.8789 ± 0.0181	0.9314 ± 0.0083	**1580 – 1590 nm**	1.0583 ± 0.0395	1.1215 ± 0.0419
920 – 930 nm	0.8692 ± 0.0184	0.9211 ± 0.0074	**1590 – 1600 nm**	1.0651 ± 0.0413	1.1287 ± 0.0441
930 – 940 nm	0.7884 ± 0.0173	0.8355 ± 0.0085	**1600 – 1610 nm**	1.0571 ± 0.0411	1.1203 ± 0.0437
940 – 950 nm	0.8515 ± 0.0188	0.9023 ± 0.0082	**1610 – 1620 nm**	1.0525 ± 0.0376	1.1154 ± 0.0403
950 – 960 nm	0.8720 ± 0.0199	0.9241 ± 0.0096	**1620 – 1630 nm**	1.0487 ± 0.0412	1.1114 ± 0.0445
960 – 970 nm	0.9161 ± 0.0211	0.9708 ± 0.0098	**1630 – 1640 nm**	1.0415 ± 0.0474	1.1037 ± 0.0514
970 – 980 nm	0.9077 ± 0.0205	0.9619 ± 0.0085	**1640 – 1650 nm**	1.0267 ± 0.0478	1.0881 ± 0.0522

4.4.2 ESA Ocean Optics RaySphere 900

Absolute Ratio R_{10}

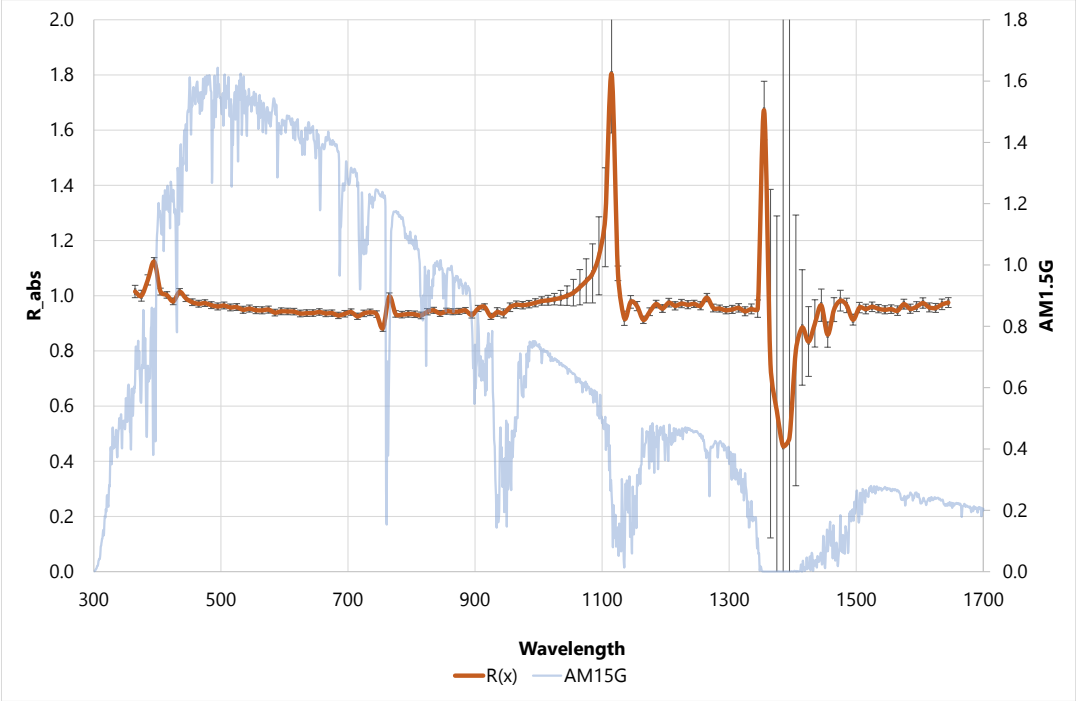

Relative Ratio R^*_{10}

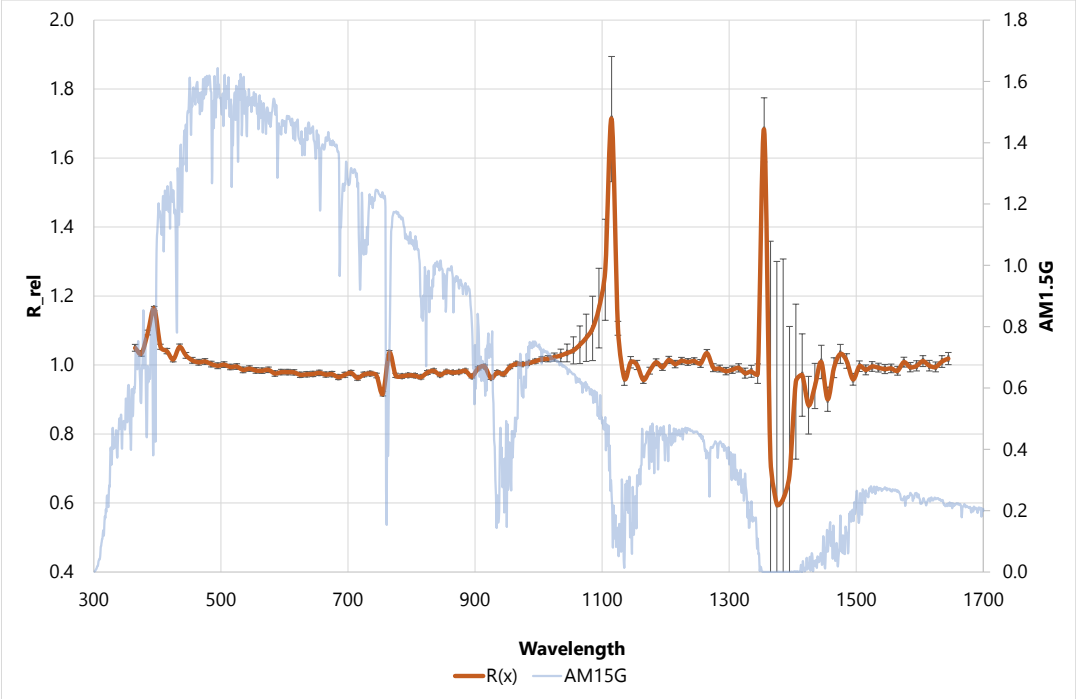

Figure 2: Performance indicators for spectroradiometer Ocean Optics RayShpere 900 (European Space Agency)

Table 6: Tabulated values of performance indicators for Ocean Optics RaySphere 900 (European Space Agency)

λ	R10 absolute	R10 relative	λ	R10 absolute	R10 relative
360 - 370 nm	1.0152 ± 0.0228	1.0498 ± 0.0103	**1010 - 1020 nm**	0.9831 ± 0.0175	1.0181 ± 0.0092
370 - 380 nm	0.9999 ± 0.0198	1.0337 ± 0.0083	**1020 - 1030 nm**	0.9875 ± 0.0206	1.0231 ± 0.0120
380 - 390 nm	1.0573 ± 0.0194	1.0941 ± 0.0077	**1030 - 1040 nm**	0.9922 ± 0.0264	1.0277 ± 0.0190
390 - 400 nm	1.1230 ± 0.0166	1.1639 ± 0.0070	**1040 - 1050 nm**	1.0003 ± 0.0354	1.0351 ± 0.0266
400 - 410 nm	1.0148 ± 0.0125	1.0527 ± 0.0078	**1050 - 1060 nm**	1.0111 ± 0.0489	1.0425 ± 0.0409
410 - 420 nm	1.0025 ± 0.0119	1.0404 ± 0.0079	**1060 - 1070 nm**	1.0310 ± 0.0659	1.0588 ± 0.0580
420 - 430 nm	0.9794 ± 0.0117	1.0163 ± 0.0074	**1070 - 1080 nm**	1.0535 ± 0.0841	1.0790 ± 0.0739
430 - 440 nm	1.0142 ± 0.0119	1.0527 ± 0.0082	**1080 - 1090 nm**	1.0810 ± 0.1156	1.1062 ± 0.1033
440 - 450 nm	0.9903 ± 0.0116	1.0279 ± 0.0085	**1090 - 1100 nm**	1.1445 ± 0.1621	1.1651 ± 0.1346
450 - 460 nm	0.9764 ± 0.0116	1.0138 ± 0.0084	**1100 - 1110 nm**	1.2843 ± 0.2302	1.2761 ± 0.1871
460 - 470 nm	0.9709 ± 0.0118	1.0081 ± 0.0086	**1110 - 1120 nm**	1.8020 ± 0.3826	1.7130 ± 0.3111
470 - 480 nm	0.9731 ± 0.0118	1.0104 ± 0.0084	**1120 - 1130 nm**	1.0812 ± 0.0284	1.1062 ± 0.0222
480 - 490 nm	0.9658 ± 0.0119	1.0028 ± 0.0083	**1130 - 1140 nm**	0.9178 ± 0.0237	0.9614 ± 0.0196
490 - 500 nm	0.9611 ± 0.0120	0.9980 ± 0.0083	**1140 - 1150 nm**	0.9775 ± 0.0225	1.0080 ± 0.0168
500 - 510 nm	0.9643 ± 0.0119	1.0012 ± 0.0083	**1150 - 1160 nm**	0.9622 ± 0.0162	1.0000 ± 0.0132
510 - 520 nm	0.9576 ± 0.0118	0.9944 ± 0.0080	**1160 - 1170 nm**	0.9125 ± 0.0123	0.9571 ± 0.0101
520 - 530 nm	0.9587 ± 0.0119	0.9956 ± 0.0080	**1170 - 1180 nm**	0.9421 ± 0.0132	0.9838 ± 0.0098
530 - 540 nm	0.9492 ± 0.0121	0.9858 ± 0.0079	**1180 - 1190 nm**	0.9698 ± 0.0133	1.0079 ± 0.0099
540 - 550 nm	0.9531 ± 0.0122	0.9897 ± 0.0080	**1190 - 1200 nm**	0.9534 ± 0.0136	0.9937 ± 0.0092
550 - 560 nm	0.9478 ± 0.0121	0.9842 ± 0.0080	**1200 - 1210 nm**	0.9747 ± 0.0151	1.0148 ± 0.0103
560 - 570 nm	0.9470 ± 0.0121	0.9836 ± 0.0079	**1210 - 1220 nm**	0.9634 ± 0.0144	1.0026 ± 0.0107
570 - 580 nm	0.9496 ± 0.0121	0.9861 ± 0.0078	**1220 - 1230 nm**	0.9714 ± 0.0145	1.0122 ± 0.0100
580 - 590 nm	0.9387 ± 0.0116	0.9755 ± 0.0076	**1230 - 1240 nm**	0.9673 ± 0.0143	1.0088 ± 0.0097
590 - 600 nm	0.9435 ± 0.0116	0.9795 ± 0.0079	**1240 - 1250 nm**	0.9704 ± 0.0127	1.0116 ± 0.0096
600 - 610 nm	0.9429 ± 0.0113	0.9794 ± 0.0078	**1250 - 1260 nm**	0.9634 ± 0.0140	1.0045 ± 0.0116
610 - 620 nm	0.9424 ± 0.0112	0.9789 ± 0.0075	**1260 - 1270 nm**	0.9930 ± 0.0149	1.0346 ± 0.0106
620 - 630 nm	0.9354 ± 0.0112	0.9717 ± 0.0074	**1270 - 1280 nm**	0.9554 ± 0.0132	0.9923 ± 0.0112
630 - 640 nm	0.9368 ± 0.0112	0.9732 ± 0.0076	**1280 - 1290 nm**	0.9535 ± 0.0123	0.9897 ± 0.0100
640 - 650 nm	0.9372 ± 0.0111	0.9740 ± 0.0074	**1290 - 1300 nm**	0.9474 ± 0.0125	0.9824 ± 0.0105
650 - 660 nm	0.9408 ± 0.0112	0.9774 ± 0.0073	**1300 - 1310 nm**	0.9503 ± 0.0140	0.9866 ± 0.0105
660 - 670 nm	0.9359 ± 0.0109	0.9724 ± 0.0073	**1310 - 1320 nm**	0.9558 ± 0.0148	0.9918 ± 0.0120
670 - 680 nm	0.9370 ± 0.0109	0.9736 ± 0.0074	**1320 - 1330 nm**	0.9435 ± 0.0154	0.9765 ± 0.0142
680 - 690 nm	0.9284 ± 0.0107	0.9650 ± 0.0069	**1330 - 1340 nm**	0.9522 ± 0.0172	0.9818 ± 0.0170
690 - 700 nm	0.9345 ± 0.0108	0.9716 ± 0.0071	**1340 - 1350 nm**	0.9533 ± 0.0300	0.9750 ± 0.0277
700 - 710 nm	0.9407 ± 0.0108	0.9773 ± 0.0069	**1350 - 1360 nm**	1.6709 ± 0.1770	1.6817 ± 0.1562
710 - 720 nm	0.9253 ± 0.0106	0.9628 ± 0.0065	**1360 - 1370 nm**	0.7538 ± 0.4760	0.7301 ± 0.4592
720 - 730 nm	0.9360 ± 0.0109	0.9727 ± 0.0063	**1370 - 1380 nm**	0.5838 ± 0.4117	0.5972 ± 0.4198
730 - 740 nm	0.9396 ± 0.0113	0.9753 ± 0.0064	**1380 - 1390 nm**	0.4549 ± 0.8301	0.6122 ± 0.4256
740 - 750 nm	0.9333 ± 0.0109	0.9696 ± 0.0065	**1390 - 1400 nm**	0.4867 ± 1.0481	0.6817 ± 0.2931
750 - 760 nm	0.8825 ± 0.0104	0.9169 ± 0.0059	**1400 - 1410 nm**	0.8019 ± 0.3931	0.9519 ± 0.2139
760 - 770 nm	0.9967 ± 0.0133	1.0355 ± 0.0065	**1410 - 1420 nm**	0.8848 ± 0.1852	0.9709 ± 0.1159

770 – 780 nm	0.9339 ± 0.0112	0.9703 ± 0.0060	**1420 – 1430 nm**	0.8340 ± 0.1054	0.8836 ± 0.0739
780 – 790 nm	0.9312 ± 0.0109	0.9679 ± 0.0060	**1430 – 1440 nm**	0.8995 ± 0.0772	0.9395 ± 0.0615
790 – 800 nm	0.9338 ± 0.0111	0.9703 ± 0.0058	**1440 – 1450 nm**	0.9652 ± 0.0565	1.0089 ± 0.0486
800 – 810 nm	0.9326 ± 0.0112	0.9693 ± 0.0058	**1450 – 1460 nm**	0.8591 ± 0.0392	0.9007 ± 0.0315
810 – 820 nm	0.9286 ± 0.0110	0.9652 ± 0.0056	**1460 – 1470 nm**	0.9494 ± 0.0410	0.9922 ± 0.0286
820 – 830 nm	0.9417 ± 0.0107	0.9783 ± 0.0055	**1470 – 1480 nm**	0.9820 ± 0.0368	1.0322 ± 0.0284
830 – 840 nm	0.9469 ± 0.0105	0.9831 ± 0.0058	**1480 – 1490 nm**	0.9648 ± 0.0252	1.0117 ± 0.0214
840 – 850 nm	0.9357 ± 0.0102	0.9717 ± 0.0054	**1490 – 1500 nm**	0.9131 ± 0.0180	0.9586 ± 0.0164
850 – 860 nm	0.9439 ± 0.0101	0.9803 ± 0.0052	**1500 – 1510 nm**	0.9568 ± 0.0180	0.9966 ± 0.0150
860 – 870 nm	0.9419 ± 0.0102	0.9784 ± 0.0051	**1510 – 1520 nm**	0.9517 ± 0.0168	0.9860 ± 0.0140
870 – 880 nm	0.9431 ± 0.0104	0.9798 ± 0.0051	**1520 – 1530 nm**	0.9599 ± 0.0166	0.9959 ± 0.0140
880 – 890 nm	0.9466 ± 0.0101	0.9831 ± 0.0051	**1530 – 1540 nm**	0.9528 ± 0.0143	0.9924 ± 0.0127
890 – 900 nm	0.9298 ± 0.0101	0.9670 ± 0.0044	**1540 – 1550 nm**	0.9490 ± 0.0140	0.9884 ± 0.0132
900 – 910 nm	0.9536 ± 0.0105	0.9902 ± 0.0043	**1550 – 1560 nm**	0.9514 ± 0.0147	0.9903 ± 0.0122
910 – 920 nm	0.9595 ± 0.0103	0.9957 ± 0.0042	**1560 – 1570 nm**	0.9458 ± 0.0164	0.9833 ± 0.0126
920 – 930 nm	0.9251 ± 0.0105	0.9626 ± 0.0041	**1570 – 1580 nm**	0.9695 ± 0.0174	1.0085 ± 0.0143
930 – 940 nm	0.9409 ± 0.0146	0.9783 ± 0.0056	**1580 – 1590 nm**	0.9525 ± 0.0158	0.9938 ± 0.0132
940 – 950 nm	0.9360 ± 0.0152	0.9739 ± 0.0057	**1590 – 1600 nm**	0.9602 ± 0.0170	0.9976 ± 0.0146
950 – 960 nm	0.9582 ± 0.0147	0.9946 ± 0.0051	**1600 – 1610 nm**	0.9733 ± 0.0184	1.0114 ± 0.0162
960 – 970 nm	0.9672 ± 0.0132	1.0036 ± 0.0053	**1610 – 1620 nm**	0.9578 ± 0.0155	0.9982 ± 0.0153
970 – 980 nm	0.9657 ± 0.0130	1.0024 ± 0.0044	**1620 – 1630 nm**	0.9557 ± 0.0154	0.9945 ± 0.0141
980 – 990 nm	0.9691 ± 0.0130	1.0063 ± 0.0046	**1630 – 1640 nm**	0.9685 ± 0.0184	1.0103 ± 0.0172
990 – 1000 nm	0.9743 ± 0.0142	1.0111 ± 0.0060	**1640 – 1650 nm**	0.9753 ± 0.0174	1.0188 ± 0.0179
1000 – 1010 nm	0.9807 ± 0.0149	1.0170 ± 0.0067			

4.4.3 PVLAB Instrument Systems CAS140

Absolute Ratio R_{10}

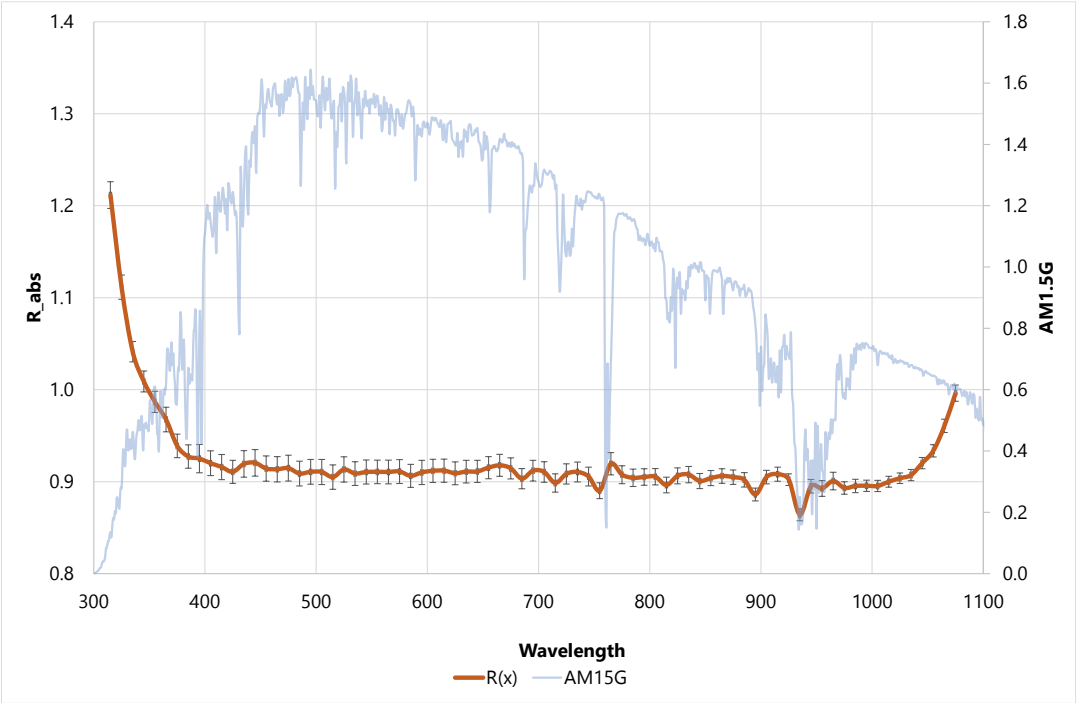

Relative Ratio R^*_{10}

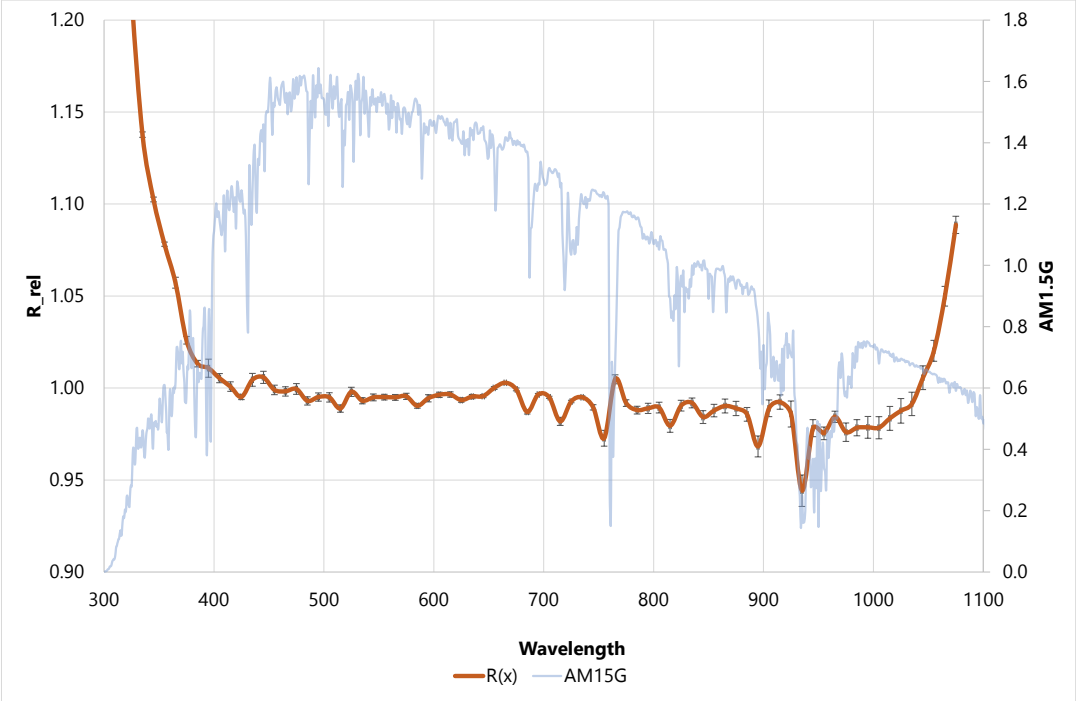

Figure 3: Performance indicators for spectroradiometer CAS140 (PVLab)

Table 7: Tabulated values of performance indicators for CAS140 (PVLab)

λ	R10 absolute	R10 relative	λ	R10 absolute	R10 relative
310 - 320 nm	1.2115 ± 0.0176	1.3238 ± 0.0074	**700 - 710 nm**	0.9105 ± 0.0101	0.9950 ± 0.0006
320 - 330 nm	1.1114 ± 0.0147	1.2144 ± 0.0048	**710 - 720 nm**	0.8986 ± 0.0090	0.9819 ± 0.0022
330 - 340 nm	1.0412 ± 0.0115	1.1377 ± 0.0017	**720 - 730 nm**	0.9084 ± 0.0099	0.9927 ± 0.0006
340 - 350 nm	1.0090 ± 0.0115	1.1025 ± 0.0014	**730 - 740 nm**	0.9105 ± 0.0099	0.9949 ± 0.0007
350 - 360 nm	0.9867 ± 0.0114	1.0781 ± 0.0012	**740 - 750 nm**	0.9055 ± 0.0092	0.9895 ± 0.0014
360 - 370 nm	0.9676 ± 0.0130	1.0572 ± 0.0031	**750 - 760 nm**	0.8901 ± 0.0077	0.9727 ± 0.0042
370 - 380 nm	0.9389 ± 0.0120	1.0259 ± 0.0021	**760 - 770 nm**	0.9195 ± 0.0111	1.0048 ± 0.0024
380 - 390 nm	0.9273 ± 0.0118	1.0133 ± 0.0018	**770 - 780 nm**	0.9076 ± 0.0088	0.9918 ± 0.0018
390 - 400 nm	0.9251 ± 0.0142	1.0108 ± 0.0050	**780 - 790 nm**	0.9041 ± 0.0086	0.9880 ± 0.0021
400 - 410 nm	0.9201 ± 0.0124	1.0053 ± 0.0025	**790 - 800 nm**	0.9050 ± 0.0082	0.9890 ± 0.0027
410 - 420 nm	0.9158 ± 0.0125	1.0007 ± 0.0026	**800 - 810 nm**	0.9054 ± 0.0080	0.9894 ± 0.0029
420 - 430 nm	0.9107 ± 0.0115	0.9951 ± 0.0014	**810 - 820 nm**	0.8963 ± 0.0076	0.9794 ± 0.0034
430 - 440 nm	0.9193 ± 0.0132	1.0045 ± 0.0035	**820 - 830 nm**	0.9063 ± 0.0079	0.9904 ± 0.0029
440 - 450 nm	0.9205 ± 0.0132	1.0058 ± 0.0034	**830 - 840 nm**	0.9077 ± 0.0080	0.9919 ± 0.0026
450 - 460 nm	0.9142 ± 0.0126	0.9990 ± 0.0026	**840 - 850 nm**	0.9007 ± 0.0074	0.9842 ± 0.0035
460 - 470 nm	0.9135 ± 0.0125	0.9982 ± 0.0025	**850 - 860 nm**	0.9039 ± 0.0074	0.9877 ± 0.0034
470 - 480 nm	0.9147 ± 0.0129	0.9995 ± 0.0029	**860 - 870 nm**	0.9061 ± 0.0072	0.9902 ± 0.0037
480 - 490 nm	0.9088 ± 0.0122	0.9930 ± 0.0022	**870 - 880 nm**	0.9049 ± 0.0071	0.9889 ± 0.0039
490 - 500 nm	0.9107 ± 0.0123	0.9951 ± 0.0022	**880 - 890 nm**	0.9020 ± 0.0071	0.9857 ± 0.0037
500 - 510 nm	0.9105 ± 0.0125	0.9949 ± 0.0025	**890 - 900 nm**	0.8860 ± 0.0061	0.9682 ± 0.0055
510 - 520 nm	0.9049 ± 0.0120	0.9888 ± 0.0020	**900 - 910 nm**	0.9050 ± 0.0066	0.9890 ± 0.0045
520 - 530 nm	0.9133 ± 0.0125	0.9980 ± 0.0025	**910 - 920 nm**	0.9081 ± 0.0070	0.9924 ± 0.0039
530 - 540 nm	0.9088 ± 0.0118	0.9931 ± 0.0017	**920 - 930 nm**	0.9022 ± 0.0057	0.9859 ± 0.0070
540 - 550 nm	0.9105 ± 0.0120	0.9949 ± 0.0019	**930 - 940 nm**	0.8640 ± 0.0056	0.9442 ± 0.0081
550 - 560 nm	0.9106 ± 0.0116	0.9951 ± 0.0015	**940 - 950 nm**	0.8951 ± 0.0065	0.9782 ± 0.0046
560 - 570 nm	0.9105 ± 0.0117	0.9949 ± 0.0016	**950 - 960 nm**	0.8926 ± 0.0077	0.9754 ± 0.0034
570 - 580 nm	0.9110 ± 0.0118	0.9955 ± 0.0017	**960 - 970 nm**	0.9008 ± 0.0086	0.9844 ± 0.0030
580 - 590 nm	0.9063 ± 0.0113	0.9903 ± 0.0013	**970 - 980 nm**	0.8931 ± 0.0061	0.9760 ± 0.0049
590 - 600 nm	0.9101 ± 0.0120	0.9944 ± 0.0020	**980 - 990 nm**	0.8953 ± 0.0064	0.9784 ± 0.0043
600 - 610 nm	0.9118 ± 0.0116	0.9963 ± 0.0014	**990 - 1000 nm**	0.8955 ± 0.0055	0.9786 ± 0.0058
610 - 620 nm	0.9119 ± 0.0116	0.9965 ± 0.0014	**1000 - 1010 nm**	0.8953 ± 0.0055	0.9784 ± 0.0059
620 - 630 nm	0.9092 ± 0.0113	0.9934 ± 0.0012	**1010 - 1020 nm**	0.9000 ± 0.0053	0.9835 ± 0.0064
630 - 640 nm	0.9109 ± 0.0113	0.9954 ± 0.0011	**1020 - 1030 nm**	0.9037 ± 0.0052	0.9876 ± 0.0066
640 - 650 nm	0.9111 ± 0.0110	0.9956 ± 0.0008	**1030 - 1040 nm**	0.9071 ± 0.0055	0.9913 ± 0.0063
650 - 660 nm	0.9152 ± 0.0109	1.0001 ± 0.0008	**1040 - 1050 nm**	0.9202 ± 0.0056	1.0056 ± 0.0065
660 - 670 nm	0.9177 ± 0.0109	1.0028 ± 0.0007	**1050 - 1060 nm**	0.9336 ± 0.0062	1.0202 ± 0.0058
670 - 680 nm	0.9145 ± 0.0105	0.9993 ± 0.0008	**1060 - 1070 nm**	0.9607 ± 0.0069	1.0499 ± 0.0056
680 - 690 nm	0.9032 ± 0.0099	0.9870 ± 0.0011	**1070 - 1080 nm**	0.9963 ± 0.0088	1.0887 ± 0.0051
690 - 700 nm	0.9119 ± 0.0103	0.9965 ± 0.0006			

4.4.4 SERIS Avantes Avaspec

Absolute Ratio R_{10}

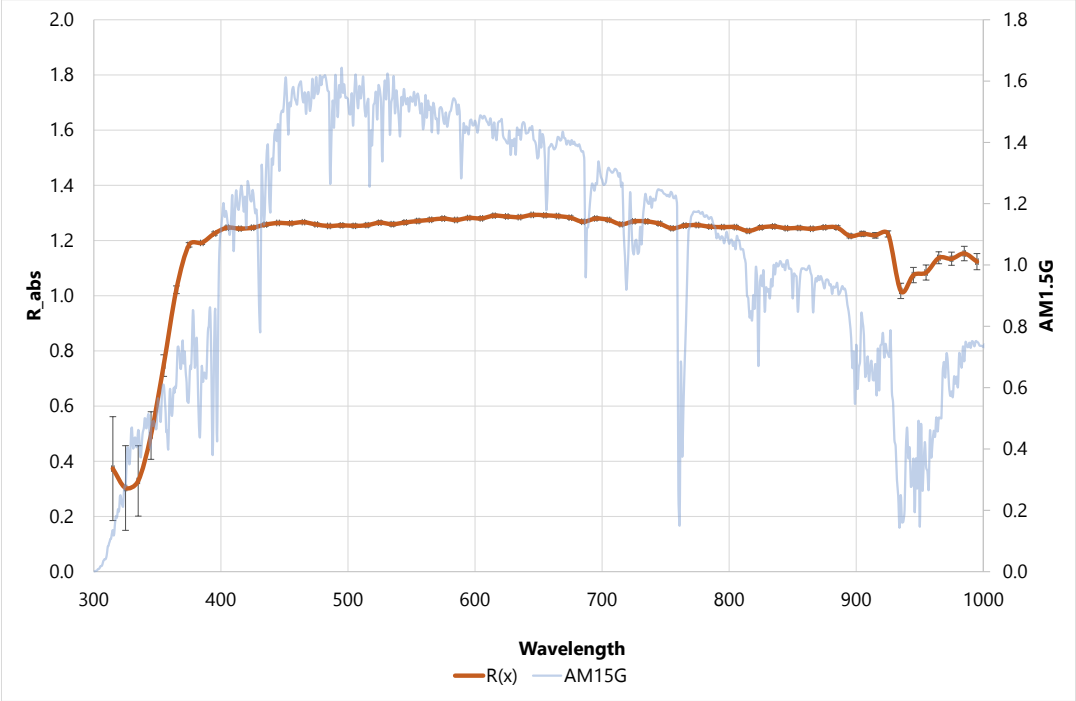

Relative Ratio R^*_{10}

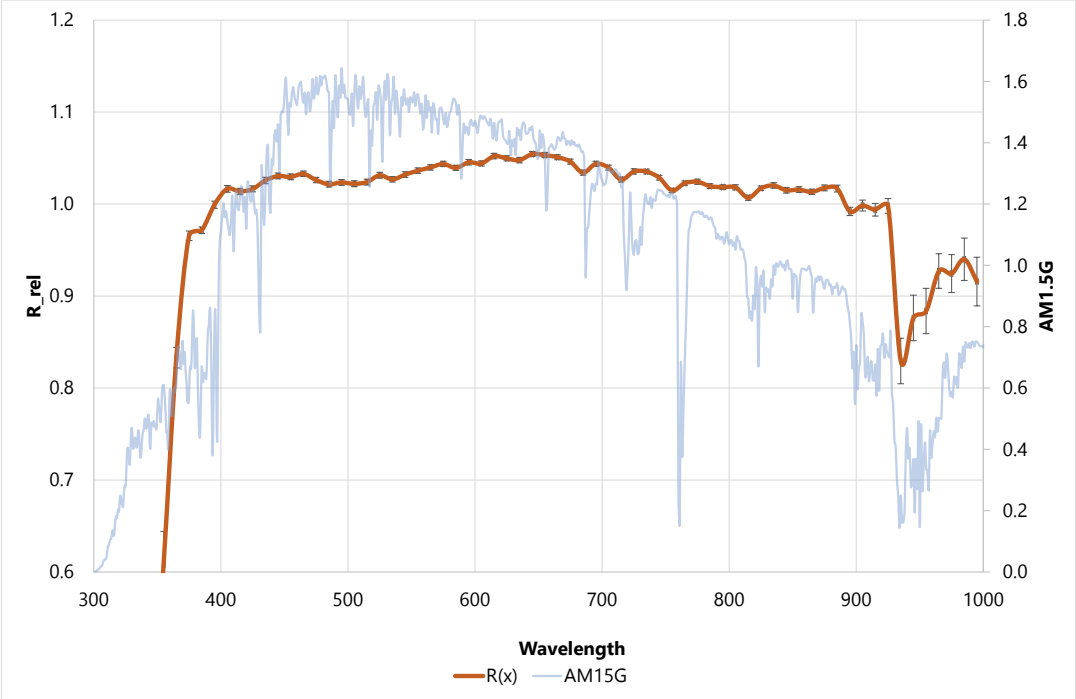

Figure 4: performance indicators for spectroradiometer Avantes Avaspec (SERIS)

Table 8: tabulated values of performance indicators for Avantes Avaspec (SERIS)

λ	R10 absolute	R10 relative	λ	R10 absolute	R10 relative
310 - 320 nm	0.3736 ± 0.0703	0.3038 ± 0.0563	**660 - 670 nm**	1.2886 ± 0.0079	1.0509 ± 0.0027
320 - 330 nm	0.3031 ± 0.0464	0.2466 ± 0.0370	**670 - 680 nm**	1.2828 ± 0.0079	1.0462 ± 0.0028
330 - 340 nm	0.3288 ± 0.0419	0.2676 ± 0.0333	**680 - 690 nm**	1.2679 ± 0.0078	1.0341 ± 0.0029
340 - 350 nm	0.4935 ± 0.0426	0.4018 ± 0.0335	**690 - 700 nm**	1.2798 ± 0.0079	1.0438 ± 0.0029
350 - 360 nm	0.7467 ± 0.0292	0.6084 ± 0.0218	**700 - 710 nm**	1.2748 ± 0.0079	1.0397 ± 0.0028
360 - 370 nm	1.0217 ± 0.0144	0.8330 ± 0.0093	**710 - 720 nm**	1.2587 ± 0.0079	1.0266 ± 0.0028
370 - 380 nm	1.1841 ± 0.0096	0.9655 ± 0.0050	**720 - 730 nm**	1.2695 ± 0.0079	1.0354 ± 0.0030
380 - 390 nm	1.1914 ± 0.0064	0.9716 ± 0.0034	**730 - 740 nm**	1.2694 ± 0.0079	1.0353 ± 0.0027
390 - 400 nm	1.2254 ± 0.0070	0.9993 ± 0.0040	**740 - 750 nm**	1.2612 ± 0.0079	1.0287 ± 0.0026
400 - 410 nm	1.2464 ± 0.0072	1.0165 ± 0.0037	**750 - 760 nm**	1.2442 ± 0.0077	1.0147 ± 0.0024
410 - 420 nm	1.2430 ± 0.0072	1.0137 ± 0.0035	**760 - 770 nm**	1.2540 ± 0.0081	1.0227 ± 0.0025
420 - 430 nm	1.2463 ± 0.0072	1.0165 ± 0.0033	**770 - 780 nm**	1.2559 ± 0.0078	1.0243 ± 0.0028
430 - 440 nm	1.2576 ± 0.0074	1.0256 ± 0.0036	**780 - 790 nm**	1.2500 ± 0.0078	1.0195 ± 0.0026
440 - 450 nm	1.2636 ± 0.0074	1.0305 ± 0.0033	**790 - 800 nm**	1.2487 ± 0.0077	1.0184 ± 0.0026
450 - 460 nm	1.2624 ± 0.0074	1.0295 ± 0.0032	**800 - 810 nm**	1.2484 ± 0.0080	1.0182 ± 0.0028
460 - 470 nm	1.2665 ± 0.0073	1.0329 ± 0.0030	**810 - 820 nm**	1.2345 ± 0.0079	1.0069 ± 0.0028
470 - 480 nm	1.2582 ± 0.0071	1.0261 ± 0.0030	**820 - 830 nm**	1.2472 ± 0.0081	1.0172 ± 0.0025
480 - 490 nm	1.2526 ± 0.0077	1.0216 ± 0.0032	**830 - 840 nm**	1.2509 ± 0.0080	1.0202 ± 0.0030
490 - 500 nm	1.2551 ± 0.0083	1.0236 ± 0.0032	**840 - 850 nm**	1.2446 ± 0.0079	1.0150 ± 0.0031
500 - 510 nm	1.2532 ± 0.0085	1.0220 ± 0.0033	**850 - 860 nm**	1.2455 ± 0.0081	1.0158 ± 0.0032
510 - 520 nm	1.2555 ± 0.0083	1.0239 ± 0.0032	**860 - 870 nm**	1.2424 ± 0.0081	1.0133 ± 0.0029
520 - 530 nm	1.2646 ± 0.0086	1.0314 ± 0.0033	**870 - 880 nm**	1.2477 ± 0.0083	1.0176 ± 0.0032
530 - 540 nm	1.2591 ± 0.0091	1.0269 ± 0.0031	**880 - 890 nm**	1.2468 ± 0.0081	1.0168 ± 0.0037
540 - 550 nm	1.2654 ± 0.0087	1.0320 ± 0.0032	**890 - 900 nm**	1.2164 ± 0.0087	0.9920 ± 0.0045
550 - 560 nm	1.2706 ± 0.0086	1.0363 ± 0.0032	**900 - 910 nm**	1.2242 ± 0.0106	0.9984 ± 0.0059
560 - 570 nm	1.2751 ± 0.0082	1.0399 ± 0.0030	**910 - 920 nm**	1.2186 ± 0.0118	0.9938 ± 0.0069
570 - 580 nm	1.2796 ± 0.0080	1.0436 ± 0.0030	**920 - 930 nm**	1.2238 ± 0.0135	0.9980 ± 0.0080
580 - 590 nm	1.2744 ± 0.0079	1.0394 ± 0.0029	**930 - 940 nm**	1.0173 ± 0.0281	0.8294 ± 0.0205
590 - 600 nm	1.2819 ± 0.0079	1.0455 ± 0.0031	**940 - 950 nm**	1.0747 ± 0.0301	0.8762 ± 0.0217
600 - 610 nm	1.2802 ± 0.0078	1.0441 ± 0.0029	**950 - 960 nm**	1.0840 ± 0.0299	0.8838 ± 0.0218
610 - 620 nm	1.2900 ± 0.0078	1.0521 ± 0.0031	**960 - 970 nm**	1.1372 ± 0.0247	0.9272 ± 0.0174
620 - 630 nm	1.2870 ± 0.0078	1.0497 ± 0.0029	**970 - 980 nm**	1.1338 ± 0.0270	0.9244 ± 0.0191
630 - 640 nm	1.2847 ± 0.0079	1.0478 ± 0.0031	**980 - 990 nm**	1.1530 ± 0.0301	0.9400 ± 0.0217
640 - 650 nm	1.2928 ± 0.0078	1.0544 ± 0.0028	**990 - 1000 nm**	1.1233 ± 0.0331	0.9157 ± 0.0242
650 - 660 nm	1.2914 ± 0.0080	1.0532 ± 0.0029			

4.4.5 SUPSI Avantes Avaspec

Absolute Ratio R_{10}

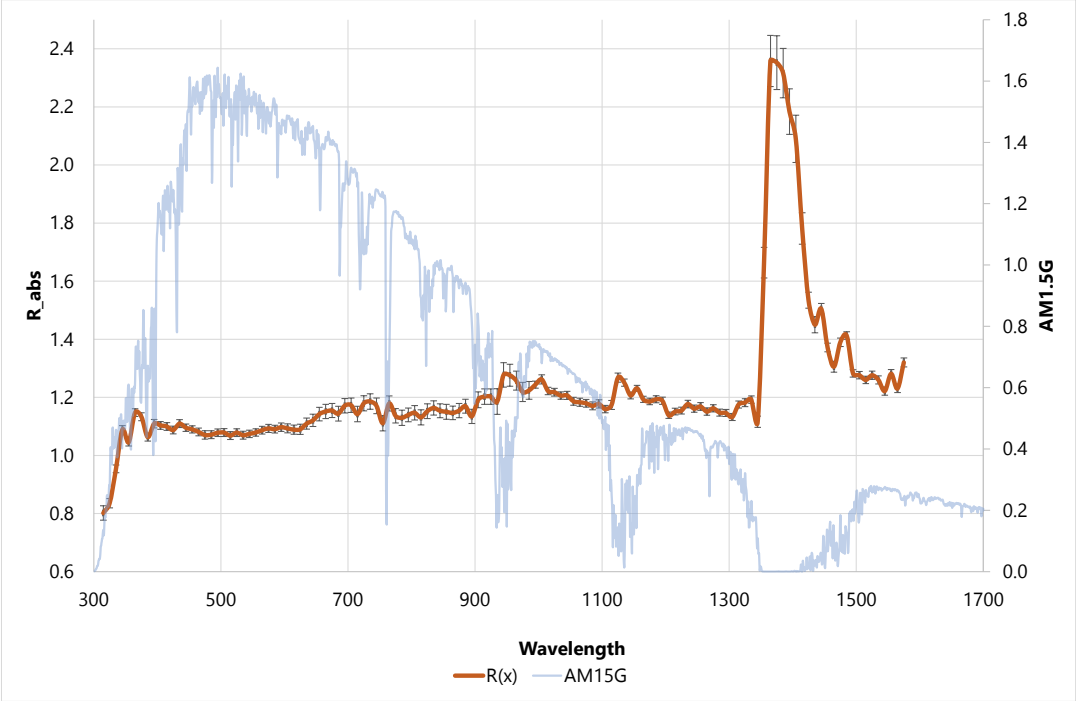

Relative Ratio R^*_{10}

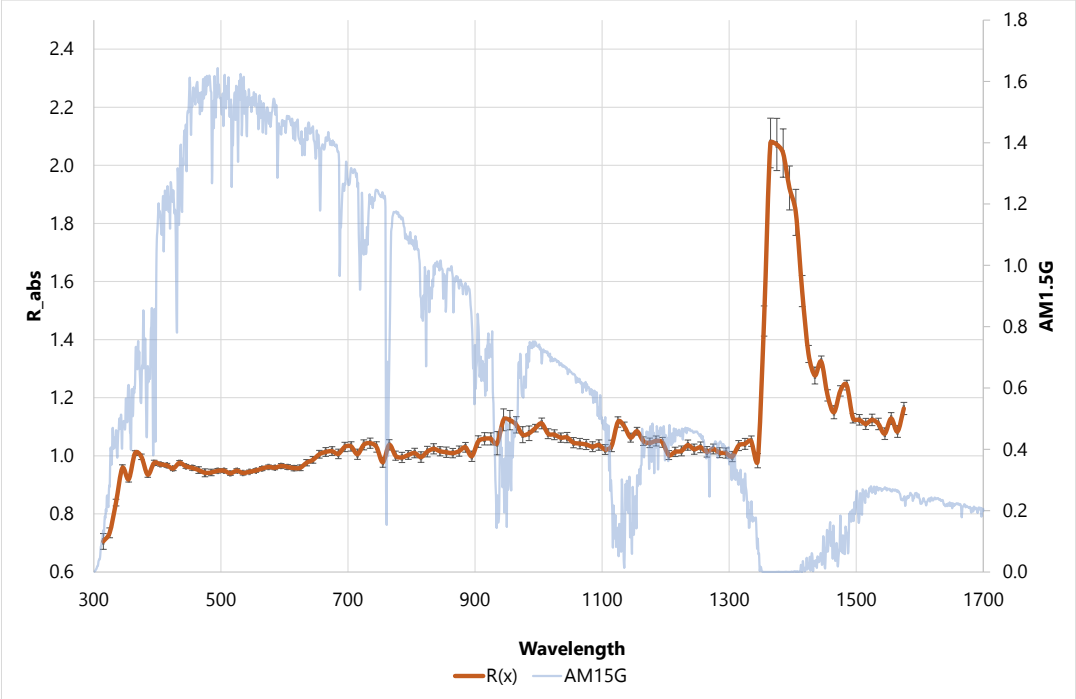

Figure 5: performance indicators for spetroradiometer Avantes Avaspec (SUPSI)

Table 9: tabulated values of performance indicators for Avantes Avaspec (SUPSI)

λ	R10 absolute	R10 relative	λ	R10 absolute	R10 relative
310 - 320 nm	0.8019 ± 0.0199	0.7055 ± 0.0192	**950 - 960 nm**	1.2760 ± 0.0482	1.1227 ± 0.0375
320 - 330 nm	0.8356 ± 0.0133	0.7349 ± 0.0124	**960 - 970 nm**	1.2574 ± 0.0411	1.1068 ± 0.0311
330 - 340 nm	0.9538 ± 0.0129	0.8387 ± 0.0096	**970 - 980 nm**	1.2186 ± 0.0400	1.0728 ± 0.0294
340 - 350 nm	1.0889 ± 0.0153	0.9576 ± 0.0111	**980 - 990 nm**	1.2239 ± 0.0375	1.0774 ± 0.0271
350 - 360 nm	1.0453 ± 0.0135	0.9192 ± 0.0089	**990 - 1000 nm**	1.2436 ± 0.0150	1.0952 ± 0.0141
360 - 370 nm	1.1476 ± 0.0153	1.0091 ± 0.0083	**1000 - 1010 nm**	1.2620 ± 0.0200	1.1116 ± 0.0206
370 - 380 nm	1.1334 ± 0.0156	0.9966 ± 0.0093	**1010 - 1020 nm**	1.2220 ± 0.0158	1.0763 ± 0.0182
380 - 390 nm	1.0633 ± 0.0148	0.9350 ± 0.0084	**1020 - 1030 nm**	1.2178 ± 0.0163	1.0726 ± 0.0181
390 - 400 nm	1.1094 ± 0.0160	0.9755 ± 0.0090	**1030 - 1040 nm**	1.2063 ± 0.0151	1.0625 ± 0.0169
400 - 410 nm	1.1036 ± 0.0146	0.9705 ± 0.0064	**1040 - 1050 nm**	1.2067 ± 0.0167	1.0629 ± 0.0185
410 - 420 nm	1.0999 ± 0.0145	0.9672 ± 0.0067	**1050 - 1060 nm**	1.1867 ± 0.0161	1.0452 ± 0.0185
420 - 430 nm	1.0875 ± 0.0143	0.9563 ± 0.0071	**1060 - 1070 nm**	1.1832 ± 0.0162	1.0421 ± 0.0185
430 - 440 nm	1.1096 ± 0.0150	0.9757 ± 0.0074	**1070 - 1080 nm**	1.1796 ± 0.0154	1.0389 ± 0.0177
440 - 450 nm	1.0957 ± 0.0140	0.9636 ± 0.0065	**1080 - 1090 nm**	1.1707 ± 0.0157	1.0312 ± 0.0175
450 - 460 nm	1.0899 ± 0.0136	0.9586 ± 0.0079	**1090 - 1100 nm**	1.1774 ± 0.0164	1.0370 ± 0.0185
460 - 470 nm	1.0812 ± 0.0144	0.9510 ± 0.0108	**1100 - 1110 nm**	1.1597 ± 0.0145	1.0215 ± 0.0173
470 - 480 nm	1.0705 ± 0.0156	0.9416 ± 0.0127	**1110 - 1120 nm**	1.1738 ± 0.0180	1.0339 ± 0.0202
480 - 490 nm	1.0716 ± 0.0146	0.9425 ± 0.0105	**1120 - 1130 nm**	1.2678 ± 0.0200	1.1165 ± 0.0200
490 - 500 nm	1.0782 ± 0.0139	0.9483 ± 0.0075	**1130 - 1140 nm**	1.2506 ± 0.0156	1.1013 ± 0.0165
500 - 510 nm	1.0789 ± 0.0146	0.9488 ± 0.0063	**1140 - 1150 nm**	1.2067 ± 0.0144	1.0627 ± 0.0163
510 - 520 nm	1.0684 ± 0.0144	0.9396 ± 0.0065	**1150 - 1160 nm**	1.2314 ± 0.0119	1.0844 ± 0.0145
520 - 530 nm	1.0788 ± 0.0144	0.9487 ± 0.0067	**1160 - 1170 nm**	1.1930 ± 0.0127	1.0506 ± 0.0156
530 - 540 nm	1.0697 ± 0.0144	0.9408 ± 0.0064	**1170 - 1180 nm**	1.1859 ± 0.0136	1.0444 ± 0.0171
540 - 550 nm	1.0744 ± 0.0136	0.9449 ± 0.0055	**1180 - 1190 nm**	1.1934 ± 0.0144	1.0510 ± 0.0179
550 - 560 nm	1.0792 ± 0.0139	0.9492 ± 0.0060	**1190 - 1200 nm**	1.1882 ± 0.0146	1.0465 ± 0.0176
560 - 570 nm	1.0871 ± 0.0143	0.9561 ± 0.0066	**1200 - 1210 nm**	1.1383 ± 0.0125	1.0025 ± 0.0157
570 - 580 nm	1.0932 ± 0.0151	0.9615 ± 0.0067	**1210 - 1220 nm**	1.1509 ± 0.0132	1.0137 ± 0.0162
580 - 590 nm	1.0906 ± 0.0148	0.9592 ± 0.0065	**1220 - 1230 nm**	1.1545 ± 0.0136	1.0168 ± 0.0172
590 - 600 nm	1.0973 ± 0.0157	0.9650 ± 0.0079	**1230 - 1240 nm**	1.1769 ± 0.0151	1.0366 ± 0.0182
600 - 610 nm	1.0934 ± 0.0167	0.9616 ± 0.0080	**1240 - 1250 nm**	1.1612 ± 0.0144	1.0227 ± 0.0180
610 - 620 nm	1.0888 ± 0.0174	0.9577 ± 0.0087	**1250 - 1260 nm**	1.1686 ± 0.0154	1.0293 ± 0.0188
620 - 630 nm	1.0901 ± 0.0193	0.9589 ± 0.0092	**1260 - 1270 nm**	1.1510 ± 0.0146	1.0138 ± 0.0181
630 - 640 nm	1.1095 ± 0.0212	0.9761 ± 0.0107	**1270 - 1280 nm**	1.1623 ± 0.0142	1.0237 ± 0.0174
640 - 650 nm	1.1209 ± 0.0237	0.9862 ± 0.0114	**1280 - 1290 nm**	1.1476 ± 0.0138	1.0107 ± 0.0172
650 - 660 nm	1.1424 ± 0.0263	1.0051 ± 0.0135	**1290 - 1300 nm**	1.1462 ± 0.0139	1.0095 ± 0.0176
660 - 670 nm	1.1515 ± 0.0283	1.0133 ± 0.0154	**1300 - 1310 nm**	1.1325 ± 0.0135	0.9975 ± 0.0174
670 - 680 nm	1.1546 ± 0.0280	1.0160 ± 0.0153	**1310 - 1320 nm**	1.1754 ± 0.0145	1.0353 ± 0.0181
680 - 690 nm	1.1439 ± 0.0293	1.0066 ± 0.0164	**1320 - 1330 nm**	1.1820 ± 0.0161	1.0411 ± 0.0195
690 - 700 nm	1.1712 ± 0.0293	1.0306 ± 0.0165	**1330 - 1340 nm**	1.1923 ± 0.0153	1.0502 ± 0.0187
700 - 710 nm	1.1731 ± 0.0290	1.0323 ± 0.0164	**1340 - 1350 nm**	1.1161 ± 0.0213	0.9831 ± 0.0240
710 - 720 nm	1.1424 ± 0.0304	1.0054 ± 0.0175	**1350 - 1360 nm**	1.6638 ± 0.0877	1.4641 ± 0.0763

720 – 730 nm	1.1795 ± 0.0306	1.0380 ± 0.0179	**1360 – 1370 nm**	2.3579 ± 0.2070	2.0769 ± 0.1772
730 – 740 nm	1.1857 ± 0.0314	1.0434 ± 0.0184	**1370 – 1380 nm**	2.3522 ± 0.2177	2.0715 ± 0.1862
740 – 750 nm	1.1710 ± 0.0316	1.0305 ± 0.0184	**1380 – 1390 nm**	2.3163 ± 0.1971	2.0419 ± 0.1697
750 – 760 nm	1.1109 ± 0.0291	0.9777 ± 0.0167	**1390 – 1400 nm**	2.1837 ± 0.1712	1.9218 ± 0.1451
760 – 770 nm	1.1790 ± 0.0308	1.0376 ± 0.0183	**1400 – 1410 nm**	2.0898 ± 0.1701	1.8381 ± 0.1456
770 – 780 nm	1.1366 ± 0.0285	1.0003 ± 0.0158	**1410 – 1420 nm**	1.7812 ± 0.0962	1.5671 ± 0.0837
780 – 790 nm	1.1298 ± 0.0296	0.9943 ± 0.0175	**1420 – 1430 nm**	1.5345 ± 0.0424	1.3505 ± 0.0400
790 – 800 nm	1.1394 ± 0.0269	1.0028 ± 0.0153	**1430 – 1440 nm**	1.4501 ± 0.0404	1.2765 ± 0.0369
800 – 810 nm	1.1470 ± 0.0286	1.0095 ± 0.0166	**1440 – 1450 nm**	1.5049 ± 0.0273	1.3242 ± 0.0253
810 – 820 nm	1.1311 ± 0.0292	0.9956 ± 0.0178	**1450 – 1460 nm**	1.3718 ± 0.0201	1.2079 ± 0.0235
820 – 830 nm	1.1524 ± 0.0294	1.0143 ± 0.0183	**1460 – 1470 nm**	1.3055 ± 0.0247	1.1499 ± 0.0258
830 – 840 nm	1.1635 ± 0.0284	1.0240 ± 0.0178	**1470 – 1480 nm**	1.3895 ± 0.0201	1.2232 ± 0.0219
840 – 850 nm	1.1540 ± 0.0275	1.0156 ± 0.0161	**1480 – 1490 nm**	1.4128 ± 0.0181	1.2436 ± 0.0207
850 – 860 nm	1.1503 ± 0.0296	1.0125 ± 0.0180	**1490 – 1500 nm**	1.2825 ± 0.0162	1.1293 ± 0.0185
860 – 870 nm	1.1465 ± 0.0269	1.0092 ± 0.0162	**1500 – 1510 nm**	1.2764 ± 0.0160	1.1240 ± 0.0203
870 – 880 nm	1.1544 ± 0.0284	1.0161 ± 0.0178	**1510 – 1520 nm**	1.2601 ± 0.0161	1.1098 ± 0.0212
880 – 890 nm	1.1696 ± 0.0276	1.0295 ± 0.0171	**1520 – 1530 nm**	1.2761 ± 0.0178	1.1237 ± 0.0222
890 – 900 nm	1.1345 ± 0.0280	0.9986 ± 0.0178	**1530 – 1540 nm**	1.2600 ± 0.0177	1.1097 ± 0.0221
900 – 910 nm	1.1917 ± 0.0322	1.0489 ± 0.0209	**1540 – 1550 nm**	1.2217 ± 0.0175	1.0760 ± 0.0217
910 – 920 nm	1.2027 ± 0.0321	1.0587 ± 0.0226	**1550 – 1560 nm**	1.2813 ± 0.0188	1.1285 ± 0.0231
920 – 930 nm	1.2026 ± 0.0323	1.0584 ± 0.0220	**1560 – 1570 nm**	1.2303 ± 0.0174	1.0837 ± 0.0220
930 – 940 nm	1.1855 ± 0.0525	1.0435 ± 0.0415	**1570 – 1580 nm**	1.3203 ± 0.0201	1.1628 ± 0.0242
940 – 950 nm	1.2772 ± 0.0538	1.1240 ± 0.0421			

4.4.6 SUPSI EKO MS710-MS712

Absolute Ratio R_{10}

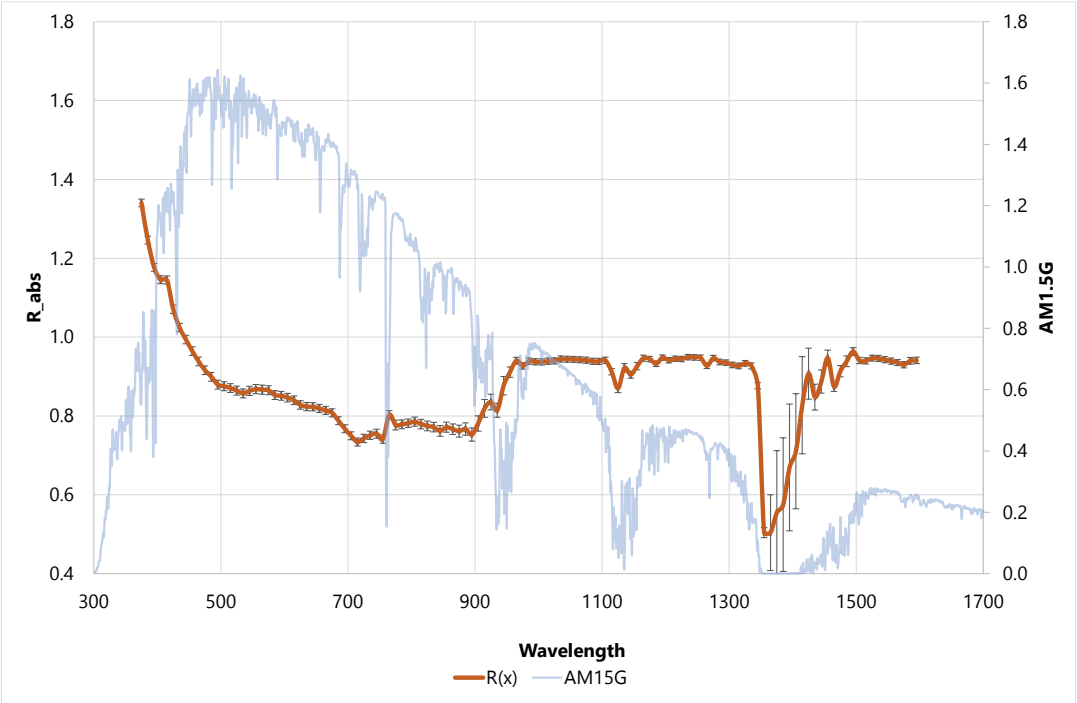

Relative Ratio R^*_{10}

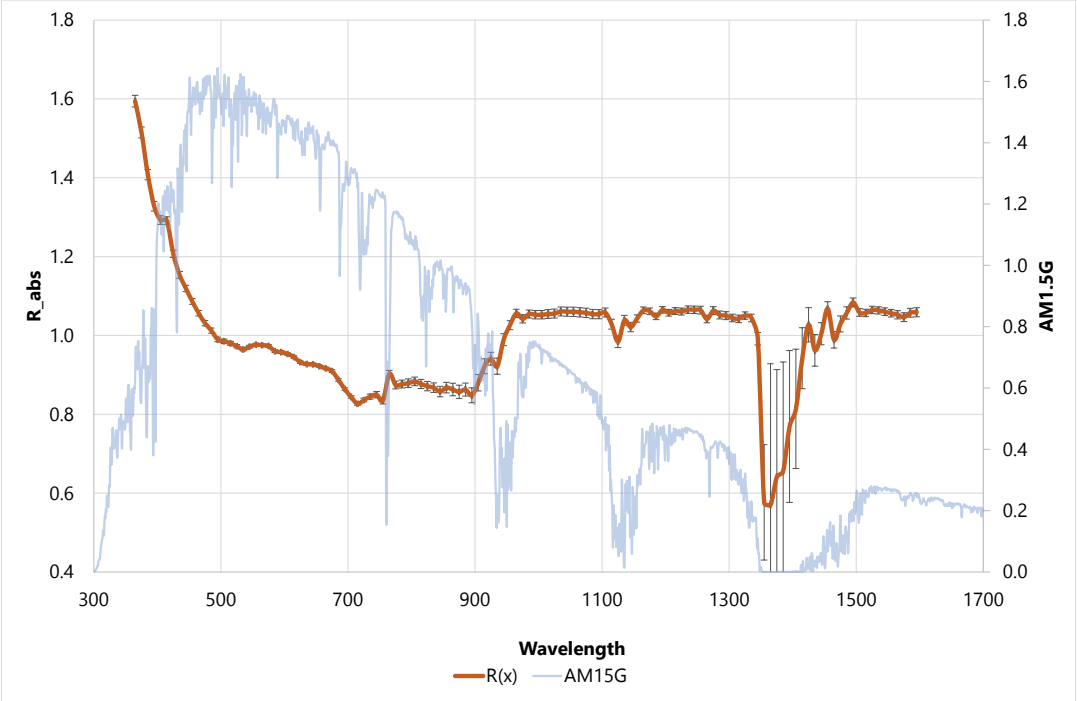

Figure 6: performance indicators for spectroradiometer EKO MS710-MS712 (SUPSI)

Table 10: tabulated values of performance indicators for MS710-MS712 (SUPSI)

λ	R10 absolute	R10 relative	λ	R10 absolute	R10 relative
360 - 370 nm	1.4100 ± 0.0136	1.5945 ± 0.0236	**980 - 990 nm**	0.9389 ± 0.0074	1.0545 ± 0.0110
370 - 380 nm	1.3404 ± 0.0133	1.5150 ± 0.0212	**990 - 1000 nm**	0.9373 ± 0.0074	1.0526 ± 0.0112
380 - 390 nm	1.2462 ± 0.0124	1.4080 ± 0.0183	**1000 - 1010 nm**	0.9371 ± 0.0075	1.0525 ± 0.0113
390 - 400 nm	1.1767 ± 0.0117	1.3278 ± 0.0161	**1010 - 1020 nm**	0.9388 ± 0.0073	1.0544 ± 0.0117
400 - 410 nm	1.1457 ± 0.0117	1.2926 ± 0.0140	**1020 - 1030 nm**	0.9397 ± 0.0073	1.0555 ± 0.0119
410 - 420 nm	1.1448 ± 0.0121	1.2910 ± 0.0128	**1030 - 1040 nm**	0.9445 ± 0.0072	1.0609 ± 0.0122
420 - 430 nm	1.0708 ± 0.0115	1.2072 ± 0.0109	**1040 - 1050 nm**	0.9439 ± 0.0072	1.0603 ± 0.0123
430 - 440 nm	1.0242 ± 0.0111	1.1536 ± 0.0099	**1050 - 1060 nm**	0.9436 ± 0.0073	1.0600 ± 0.0124
440 - 450 nm	0.9938 ± 0.0109	1.1191 ± 0.0090	**1060 - 1070 nm**	0.9426 ± 0.0073	1.0588 ± 0.0126
450 - 460 nm	0.9645 ± 0.0106	1.0862 ± 0.0080	**1070 - 1080 nm**	0.9414 ± 0.0073	1.0574 ± 0.0126
460 - 470 nm	0.9382 ± 0.0103	1.0565 ± 0.0075	**1080 - 1090 nm**	0.9387 ± 0.0073	1.0543 ± 0.0123
470 - 480 nm	0.9161 ± 0.0102	1.0312 ± 0.0070	**1090 - 1100 nm**	0.9382 ± 0.0074	1.0541 ± 0.0122
480 - 490 nm	0.8994 ± 0.0102	1.0124 ± 0.0064	**1100 - 1110 nm**	0.9413 ± 0.0077	1.0581 ± 0.0121
490 - 500 nm	0.8795 ± 0.0100	0.9899 ± 0.0058	**1110 - 1120 nm**	0.9122 ± 0.0097	1.0284 ± 0.0128
500 - 510 nm	0.8755 ± 0.0098	0.9852 ± 0.0054	**1120 - 1130 nm**	0.8700 ± 0.0093	0.9842 ± 0.0147
510 - 520 nm	0.8707 ± 0.0099	0.9801 ± 0.0048	**1130 - 1140 nm**	0.9219 ± 0.0083	1.0385 ± 0.0129
520 - 530 nm	0.8644 ± 0.0099	0.9727 ± 0.0043	**1140 - 1150 nm**	0.9048 ± 0.0082	1.0213 ± 0.0119
530 - 540 nm	0.8571 ± 0.0099	0.9645 ± 0.0037	**1150 - 1160 nm**	0.9262 ± 0.0070	1.0430 ± 0.0095
540 - 550 nm	0.8636 ± 0.0100	0.9717 ± 0.0034	**1160 - 1170 nm**	0.9466 ± 0.0064	1.0636 ± 0.0090
550 - 560 nm	0.8679 ± 0.0100	0.9766 ± 0.0034	**1170 - 1180 nm**	0.9444 ± 0.0064	1.0612 ± 0.0088
560 - 570 nm	0.8667 ± 0.0099	0.9752 ± 0.0033	**1180 - 1190 nm**	0.9323 ± 0.0063	1.0484 ± 0.0087
570 - 580 nm	0.8651 ± 0.0098	0.9734 ± 0.0032	**1190 - 1200 nm**	0.9479 ± 0.0064	1.0650 ± 0.0089
580 - 590 nm	0.8529 ± 0.0095	0.9600 ± 0.0033	**1200 - 1210 nm**	0.9414 ± 0.0063	1.0577 ± 0.0090
590 - 600 nm	0.8512 ± 0.0094	0.9578 ± 0.0033	**1210 - 1220 nm**	0.9450 ± 0.0063	1.0617 ± 0.0093
600 - 610 nm	0.8465 ± 0.0092	0.9529 ± 0.0030	**1220 - 1230 nm**	0.9445 ± 0.0063	1.0608 ± 0.0095
610 - 620 nm	0.8396 ± 0.0089	0.9452 ± 0.0031	**1230 - 1240 nm**	0.9492 ± 0.0065	1.0657 ± 0.0101
620 - 630 nm	0.8281 ± 0.0088	0.9322 ± 0.0031	**1240 - 1250 nm**	0.9486 ± 0.0065	1.0650 ± 0.0100
630 - 640 nm	0.8238 ± 0.0087	0.9274 ± 0.0030	**1250 - 1260 nm**	0.9476 ± 0.0067	1.0641 ± 0.0104
640 - 650 nm	0.8231 ± 0.0085	0.9268 ± 0.0030	**1260 - 1270 nm**	0.9272 ± 0.0065	1.0417 ± 0.0099
650 - 660 nm	0.8190 ± 0.0085	0.9219 ± 0.0029	**1270 - 1280 nm**	0.9467 ± 0.0065	1.0630 ± 0.0107
660 - 670 nm	0.8142 ± 0.0083	0.9165 ± 0.0030	**1280 - 1290 nm**	0.9370 ± 0.0064	1.0521 ± 0.0107
670 - 680 nm	0.8080 ± 0.0082	0.9095 ± 0.0031	**1290 - 1300 nm**	0.9352 ± 0.0064	1.0503 ± 0.0106
680 - 690 nm	0.7881 ± 0.0079	0.8874 ± 0.0028	**1300 - 1310 nm**	0.9294 ± 0.0065	1.0444 ± 0.0101
690 - 700 nm	0.7675 ± 0.0077	0.8640 ± 0.0028	**1310 - 1320 nm**	0.9269 ± 0.0066	1.0422 ± 0.0099
700 - 710 nm	0.7498 ± 0.0076	0.8440 ± 0.0027	**1320 - 1330 nm**	0.9335 ± 0.0070	1.0505 ± 0.0097
710 - 720 nm	0.7338 ± 0.0077	0.8267 ± 0.0032	**1330 - 1340 nm**	0.9271 ± 0.0071	1.0443 ± 0.0101
720 - 730 nm	0.7430 ± 0.0078	0.8362 ± 0.0041	**1340 - 1350 nm**	0.8768 ± 0.0113	0.9919 ± 0.0158
730 - 740 nm	0.7510 ± 0.0085	0.8448 ± 0.0053	**1350 - 1360 nm**	0.5041 ± 0.0485	0.5766 ± 0.0845
740 - 750 nm	0.7551 ± 0.0080	0.8498 ± 0.0067	**1360 - 1370 nm**	0.5041 ± 0.0792	0.5702 ± 0.2041
750 - 760 nm	0.7414 ± 0.0081	0.8349 ± 0.0073	**1370 - 1380 nm**	0.5548 ± 0.0941	0.6417 ± 0.1745
760 - 770 nm	0.8030 ± 0.0098	0.9026 ± 0.0079	**1380 - 1390 nm**	0.5751 ± 0.0924	0.6566 ± 0.1814
770 - 780 nm	0.7770 ± 0.0087	0.8743 ± 0.0084	**1390 - 1400 nm**	0.6695 ± 0.0978	0.7690 ± 0.1480

780 – 790 nm	0.7790 ± 0.0083	0.8766 ± 0.0087	**1400 – 1410 nm**	0.7105 ± 0.0876	0.8139 ± 0.1232
790 – 800 nm	0.7814 ± 0.0091	0.8789 ± 0.0096	**1410 – 1420 nm**	0.8274 ± 0.0535	0.9422 ± 0.0728
800 – 810 nm	0.7855 ± 0.0094	0.8836 ± 0.0097	**1420 – 1430 nm**	0.9073 ± 0.0296	1.0271 ± 0.0448
810 – 820 nm	0.7794 ± 0.0096	0.8771 ± 0.0101	**1430 – 1440 nm**	0.8479 ± 0.0248	0.9622 ± 0.0386
820 – 830 nm	0.7747 ± 0.0093	0.8714 ± 0.0102	**1440 – 1450 nm**	0.8873 ± 0.0177	1.0045 ± 0.0281
830 – 840 nm	0.7717 ± 0.0104	0.8678 ± 0.0104	**1450 – 1460 nm**	0.9472 ± 0.0116	1.0679 ± 0.0190
840 – 850 nm	0.7622 ± 0.0097	0.8576 ± 0.0112	**1460 – 1470 nm**	0.8743 ± 0.0124	0.9889 ± 0.0208
850 – 860 nm	0.7715 ± 0.0104	0.8677 ± 0.0115	**1470 – 1480 nm**	0.9135 ± 0.0124	1.0293 ± 0.0208
860 – 870 nm	0.7665 ± 0.0117	0.8628 ± 0.0136	**1480 – 1490 nm**	0.9389 ± 0.0095	1.0570 ± 0.0165
870 – 880 nm	0.7616 ± 0.0118	0.8570 ± 0.0145	**1490 – 1500 nm**	0.9633 ± 0.0077	1.0835 ± 0.0124
880 – 890 nm	0.7669 ± 0.0127	0.8627 ± 0.0141	**1500 – 1510 nm**	0.9406 ± 0.0074	1.0584 ± 0.0105
890 – 900 nm	0.7529 ± 0.0146	0.8482 ± 0.0162	**1510 – 1520 nm**	0.9396 ± 0.0070	1.0571 ± 0.0100
900 – 910 nm	0.7810 ± 0.0175	0.8800 ± 0.0184	**1520 – 1530 nm**	0.9467 ± 0.0075	1.0648 ± 0.0100
910 – 920 nm	0.8193 ± 0.0163	0.9219 ± 0.0174	**1530 – 1540 nm**	0.9458 ± 0.0073	1.0637 ± 0.0098
920 – 930 nm	0.8353 ± 0.0148	0.9408 ± 0.0153	**1540 – 1550 nm**	0.9427 ± 0.0074	1.0602 ± 0.0102
930 – 940 nm	0.8145 ± 0.0190	0.9221 ± 0.0188	**1550 – 1560 nm**	0.9393 ± 0.0073	1.0564 ± 0.0100
940 – 950 nm	0.8769 ± 0.0114	0.9894 ± 0.0150	**1560 – 1570 nm**	0.9354 ± 0.0073	1.0524 ± 0.0109
950 – 960 nm	0.9111 ± 0.0080	1.0263 ± 0.0117	**1570 – 1580 nm**	0.9299 ± 0.0078	1.0463 ± 0.0117
960 – 970 nm	0.9401 ± 0.0075	1.0561 ± 0.0110	**1580 – 1590 nm**	0.9399 ± 0.0076	1.0577 ± 0.0118
970 – 980 nm	0.9268 ± 0.0074	1.0421 ± 0.0110	**1590 – 1600 nm**	0.9409 ± 0.0079	1.0590 ± 0.0123

4.4.7 K. Murray EKO MS700

Absolute Ratio R_{10}

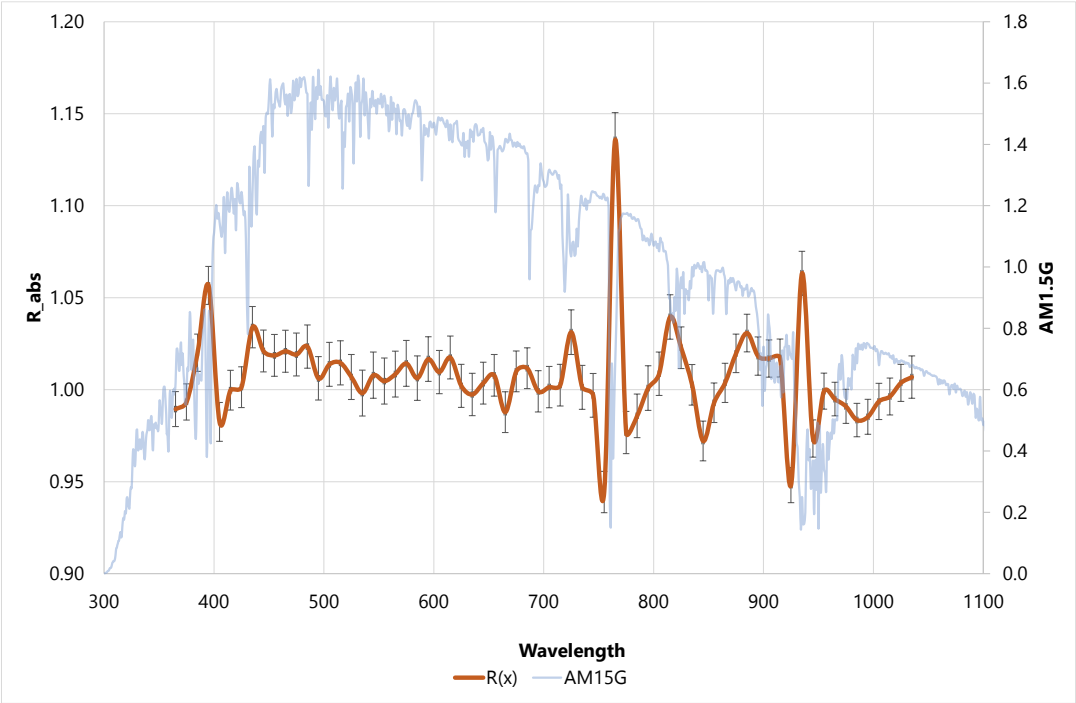

Relative Ratio R^*_{10}

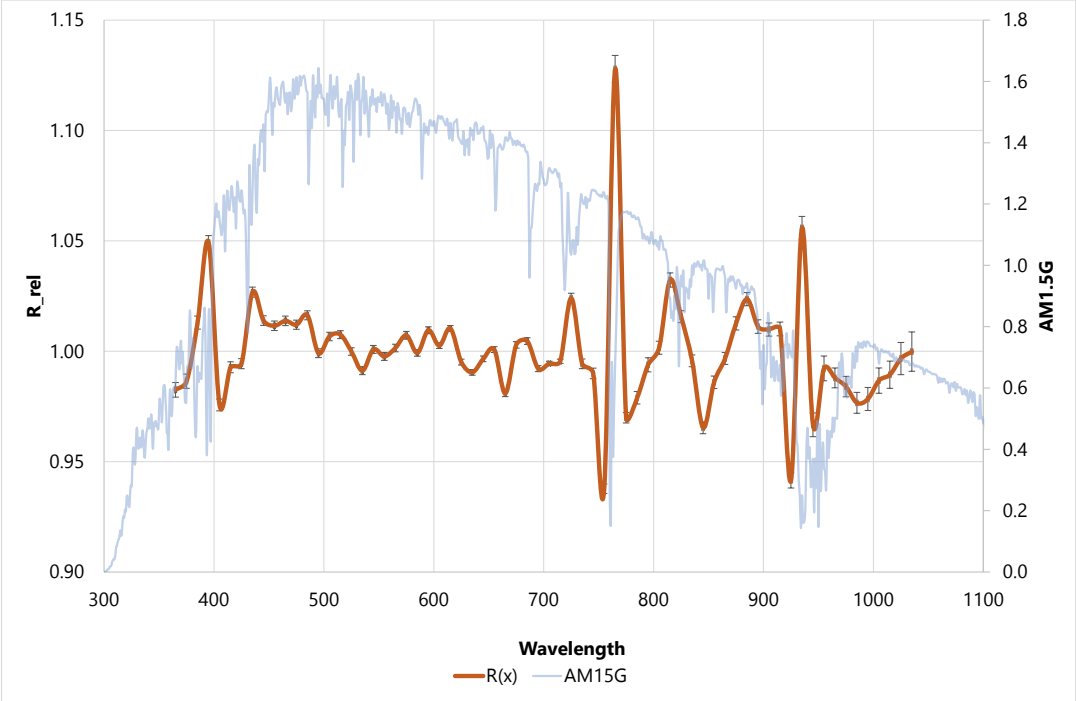

Figure 7: performance indicators for spectroradiometer EKO MS700 (North West Regional College)

Table 11: tabulated values of performance indicators for EKO MS700 (North West Regional College)

λ	R10 absolute	R10 relative	λ	R10 absolute	R10 relative
360 - 370 nm	0.9895 ± 0.0094	0.9825 ± 0.0033	**700 - 710 nm**	1.0014 ± 0.0112	0.9944 ± 0.0010
370 - 380 nm	0.9934 ± 0.0098	0.9864 ± 0.0032	**710 - 720 nm**	1.0025 ± 0.0113	0.9955 ± 0.0010
380 - 390 nm	1.0201 ± 0.0103	1.0129 ± 0.0030	**720 - 730 nm**	1.0313 ± 0.0125	1.0241 ± 0.0022
390 - 400 nm	1.0567 ± 0.0109	1.0493 ± 0.0032	**730 - 740 nm**	1.0013 ± 0.0120	0.9943 ± 0.0022
400 - 410 nm	0.9825 ± 0.0104	0.9756 ± 0.0026	**740 - 750 nm**	0.9969 ± 0.0119	0.9899 ± 0.0024
410 - 420 nm	0.9997 ± 0.0108	0.9927 ± 0.0025	**750 - 760 nm**	0.9443 ± 0.0106	0.9377 ± 0.0020
420 - 430 nm	1.0014 ± 0.0111	0.9944 ± 0.0023	**760 - 770 nm**	1.1358 ± 0.0168	1.1278 ± 0.0070
430 - 440 nm	1.0340 ± 0.0116	1.0268 ± 0.0023	**770 - 780 nm**	0.9767 ± 0.0112	0.9699 ± 0.0023
440 - 450 nm	1.0210 ± 0.0116	1.0139 ± 0.0022	**780 - 790 nm**	0.9858 ± 0.0117	0.9789 ± 0.0028
450 - 460 nm	1.0187 ± 0.0116	1.0115 ± 0.0022	**790 - 800 nm**	1.0009 ± 0.0121	0.9939 ± 0.0032
460 - 470 nm	1.0209 ± 0.0117	1.0137 ± 0.0022	**800 - 810 nm**	1.0086 ± 0.0119	1.0016 ± 0.0029
470 - 480 nm	1.0191 ± 0.0119	1.0120 ± 0.0021	**810 - 820 nm**	1.0396 ± 0.0126	1.0323 ± 0.0033
480 - 490 nm	1.0234 ± 0.0120	1.0163 ± 0.0021	**820 - 830 nm**	1.0228 ± 0.0116	1.0156 ± 0.0027
490 - 500 nm	1.0061 ± 0.0119	0.9991 ± 0.0020	**830 - 840 nm**	1.0026 ± 0.0111	0.9956 ± 0.0027
500 - 510 nm	1.0138 ± 0.0121	1.0067 ± 0.0019	**840 - 850 nm**	0.9721 ± 0.0105	0.9653 ± 0.0026
510 - 520 nm	1.0146 ± 0.0122	1.0075 ± 0.0018	**850 - 860 nm**	0.9929 ± 0.0107	0.9859 ± 0.0028
520 - 530 nm	1.0069 ± 0.0123	0.9999 ± 0.0017	**860 - 870 nm**	1.0037 ± 0.0107	0.9967 ± 0.0027
530 - 540 nm	0.9982 ± 0.0125	0.9912 ± 0.0018	**870 - 880 nm**	1.0197 ± 0.0107	1.0126 ± 0.0030
540 - 550 nm	1.0079 ± 0.0126	1.0008 ± 0.0018	**880 - 890 nm**	1.0308 ± 0.0105	1.0236 ± 0.0031
550 - 560 nm	1.0047 ± 0.0126	0.9976 ± 0.0018	**890 - 900 nm**	1.0183 ± 0.0106	1.0112 ± 0.0031
560 - 570 nm	1.0085 ± 0.0126	1.0014 ± 0.0017	**900 - 910 nm**	1.0169 ± 0.0103	1.0098 ± 0.0030
570 - 580 nm	1.0143 ± 0.0126	1.0072 ± 0.0018	**910 - 920 nm**	1.0172 ± 0.0105	1.0101 ± 0.0031
580 - 590 nm	1.0063 ± 0.0121	0.9992 ± 0.0014	**920 - 930 nm**	0.9481 ± 0.0090	0.9415 ± 0.0032
590 - 600 nm	1.0166 ± 0.0124	1.0095 ± 0.0016	**930 - 940 nm**	1.0633 ± 0.0127	1.0559 ± 0.0055
600 - 610 nm	1.0096 ± 0.0119	1.0025 ± 0.0013	**940 - 950 nm**	0.9735 ± 0.0099	0.9667 ± 0.0052
610 - 620 nm	1.0175 ± 0.0119	1.0104 ± 0.0013	**950 - 960 nm**	0.9992 ± 0.0097	0.9922 ± 0.0055
620 - 630 nm	1.0021 ± 0.0117	0.9951 ± 0.0013	**960 - 970 nm**	0.9949 ± 0.0091	0.9879 ± 0.0044
630 - 640 nm	0.9974 ± 0.0115	0.9904 ± 0.0012	**970 - 980 nm**	0.9909 ± 0.0092	0.9840 ± 0.0046
640 - 650 nm	1.0036 ± 0.0114	0.9965 ± 0.0013	**980 - 990 nm**	0.9835 ± 0.0090	0.9766 ± 0.0046
650 - 660 nm	1.0078 ± 0.0114	1.0007 ± 0.0013	**990 - 1000 nm**	0.9853 ± 0.0094	0.9784 ± 0.0051
660 - 670 nm	0.9878 ± 0.0109	0.9809 ± 0.0014	**1000 - 1010 nm**	0.9937 ± 0.0098	0.9867 ± 0.0057
670 - 680 nm	1.0100 ± 0.0112	1.0029 ± 0.0015	**1010 - 1020 nm**	0.9963 ± 0.0100	0.9893 ± 0.0061
680 - 690 nm	1.0117 ± 0.0113	1.0046 ± 0.0015	**1020 - 1030 nm**	1.0037 ± 0.0101	0.9967 ± 0.0073
690 - 700 nm	0.9991 ± 0.0112	0.9921 ± 0.0014	**1030 - 1040 nm**	1.0069 ± 0.0116	0.9998 ± 0.0089

4.5 Direct Normal Spectral Irradiance

4.5.1 RSE Spectrafy SolarSIM D2

Absolute Ratio R_{10}

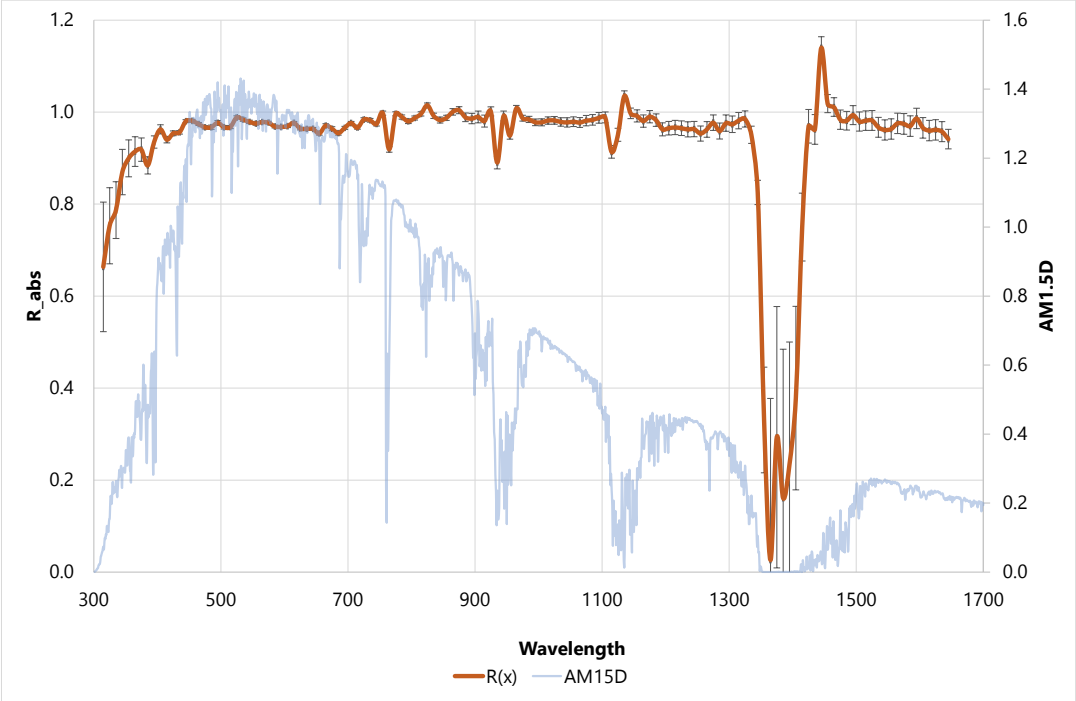

Relative Ratio R^*_{10}

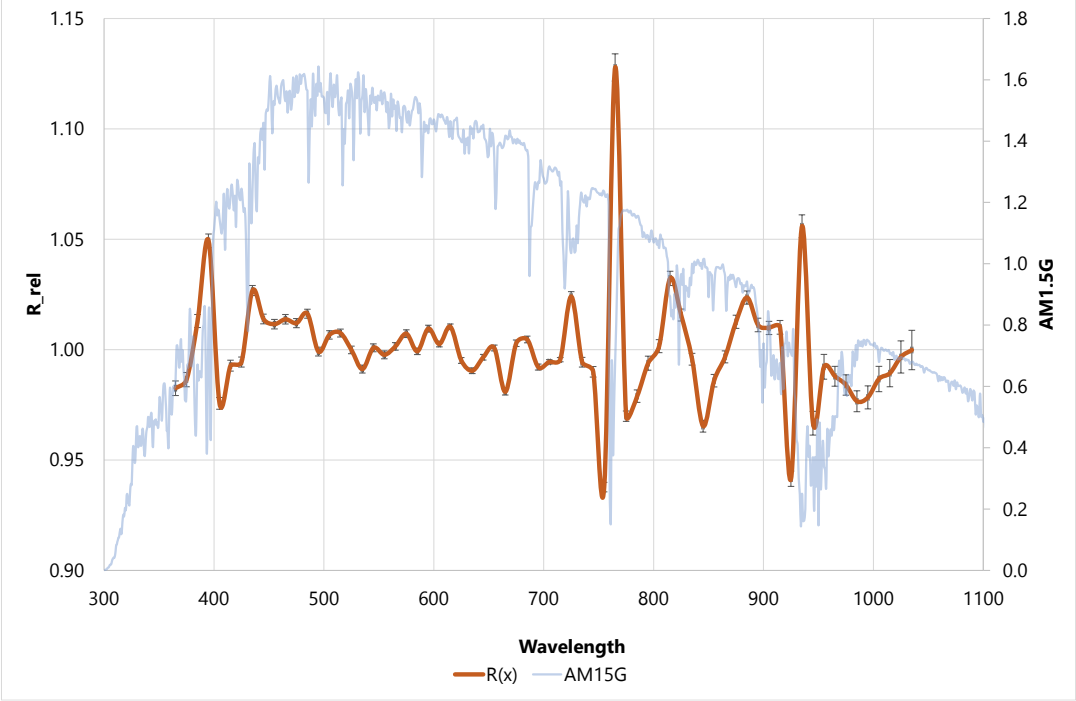

Figure 8: performance indicators for spectroradiometer Spectrafy Solar SIM D2 (RSE)

Table 12: tabulated values of performance indicators for Spectrafy Solar SIM D2 (RSE)

λ	R10 absolute	R10 relative	λ	R10 absolute	R10 relative
310 - 320 nm	0.6636 ± 0.0936	0.6833 ± 0.0934	**980 - 990 nm**	0.9842 ± 0.0065	1.0135 ± 0.0025
320 - 330 nm	0.7529 ± 0.0623	0.7753 ± 0.0606	**990 - 1000 nm**	0.9780 ± 0.0071	1.0071 ± 0.0028
330 - 340 nm	0.7870 ± 0.0486	0.8104 ± 0.0463	**1000 - 1010 nm**	0.9779 ± 0.0075	1.0071 ± 0.0033
340 - 350 nm	0.8698 ± 0.0429	0.8957 ± 0.0400	**1010 - 1020 nm**	0.9818 ± 0.0080	1.0110 ± 0.0037
350 - 360 nm	0.8996 ± 0.0362	0.9264 ± 0.0330	**1020 - 1030 nm**	0.9821 ± 0.0083	1.0114 ± 0.0040
360 - 370 nm	0.9142 ± 0.0296	0.9415 ± 0.0261	**1030 - 1040 nm**	0.9787 ± 0.0091	1.0078 ± 0.0048
370 - 380 nm	0.9184 ± 0.0233	0.9458 ± 0.0197	**1040 - 1050 nm**	0.9777 ± 0.0098	1.0069 ± 0.0055
380 - 390 nm	0.8843 ± 0.0165	0.9106 ± 0.0131	**1050 - 1060 nm**	0.9791 ± 0.0102	1.0083 ± 0.0059
390 - 400 nm	0.9350 ± 0.0125	0.9628 ± 0.0086	**1060 - 1070 nm**	0.9774 ± 0.0106	1.0066 ± 0.0063
400 - 410 nm	0.9625 ± 0.0096	0.9912 ± 0.0056	**1070 - 1080 nm**	0.9815 ± 0.0110	1.0107 ± 0.0068
410 - 420 nm	0.9402 ± 0.0066	0.9682 ± 0.0032	**1080 - 1090 nm**	0.9831 ± 0.0113	1.0124 ± 0.0071
420 - 430 nm	0.9540 ± 0.0048	0.9824 ± 0.0034	**1090 - 1100 nm**	0.9875 ± 0.0115	1.0169 ± 0.0072
430 - 440 nm	0.9561 ± 0.0038	0.9846 ± 0.0043	**1100 - 1110 nm**	0.9885 ± 0.0117	1.0179 ± 0.0074
440 - 450 nm	0.9803 ± 0.0033	1.0096 ± 0.0051	**1110 - 1120 nm**	0.9136 ± 0.0126	0.9408 ± 0.0092
450 - 460 nm	0.9810 ± 0.0032	1.0102 ± 0.0052	**1120 - 1130 nm**	0.9509 ± 0.0134	0.9791 ± 0.0113
460 - 470 nm	0.9742 ± 0.0032	1.0032 ± 0.0048	**1130 - 1140 nm**	1.0349 ± 0.0115	1.0658 ± 0.0085
470 - 480 nm	0.9670 ± 0.0035	0.9958 ± 0.0039	**1140 - 1150 nm**	0.9973 ± 0.0115	1.0270 ± 0.0080
480 - 490 nm	0.9672 ± 0.0043	0.9960 ± 0.0031	**1150 - 1160 nm**	0.9919 ± 0.0130	1.0214 ± 0.0088
490 - 500 nm	0.9770 ± 0.0046	1.0061 ± 0.0030	**1160 - 1170 nm**	0.9806 ± 0.0131	1.0098 ± 0.0090
500 - 510 nm	0.9672 ± 0.0038	0.9960 ± 0.0039	**1170 - 1180 nm**	0.9901 ± 0.0134	1.0196 ± 0.0092
510 - 520 nm	0.9676 ± 0.0034	0.9964 ± 0.0053	**1180 - 1190 nm**	0.9826 ± 0.0134	1.0119 ± 0.0093
520 - 530 nm	0.9886 ± 0.0035	1.0181 ± 0.0060	**1190 - 1200 nm**	0.9627 ± 0.0137	0.9913 ± 0.0096
530 - 540 nm	0.9838 ± 0.0036	1.0131 ± 0.0063	**1200 - 1210 nm**	0.9652 ± 0.0142	0.9939 ± 0.0102
540 - 550 nm	0.9789 ± 0.0036	1.0080 ± 0.0067	**1210 - 1220 nm**	0.9667 ± 0.0150	0.9955 ± 0.0109
550 - 560 nm	0.9753 ± 0.0035	1.0044 ± 0.0069	**1220 - 1230 nm**	0.9651 ± 0.0154	0.9938 ± 0.0114
560 - 570 nm	0.9784 ± 0.0032	1.0075 ± 0.0062	**1230 - 1240 nm**	0.9625 ± 0.0158	0.9911 ± 0.0118
570 - 580 nm	0.9772 ± 0.0030	1.0063 ± 0.0058	**1240 - 1250 nm**	0.9631 ± 0.0159	0.9918 ± 0.0119
580 - 590 nm	0.9687 ± 0.0030	0.9976 ± 0.0064	**1250 - 1260 nm**	0.9535 ± 0.0157	0.9819 ± 0.0118
590 - 600 nm	0.9680 ± 0.0028	0.9968 ± 0.0059	**1260 - 1270 nm**	0.9624 ± 0.0163	0.9911 ± 0.0124
600 - 610 nm	0.9694 ± 0.0028	0.9983 ± 0.0048	**1270 - 1280 nm**	0.9770 ± 0.0165	1.0061 ± 0.0125
610 - 620 nm	0.9768 ± 0.0028	1.0059 ± 0.0051	**1280 - 1290 nm**	0.9588 ± 0.0166	0.9874 ± 0.0127
620 - 630 nm	0.9642 ± 0.0028	0.9930 ± 0.0049	**1290 - 1300 nm**	0.9761 ± 0.0174	1.0052 ± 0.0134
630 - 640 nm	0.9636 ± 0.0030	0.9923 ± 0.0046	**1300 - 1310 nm**	0.9736 ± 0.0175	1.0026 ± 0.0135
640 - 650 nm	0.9638 ± 0.0031	0.9925 ± 0.0044	**1310 - 1320 nm**	0.9815 ± 0.0174	1.0107 ± 0.0135
650 - 660 nm	0.9536 ± 0.0033	0.9820 ± 0.0039	**1320 - 1330 nm**	0.9851 ± 0.0174	1.0144 ± 0.0134
660 - 670 nm	0.9708 ± 0.0039	0.9998 ± 0.0032	**1330 - 1340 nm**	0.9507 ± 0.0179	0.9789 ± 0.0141
670 - 680 nm	0.9638 ± 0.0043	0.9926 ± 0.0029	**1340 - 1350 nm**	0.8254 ± 0.0219	0.8498 ± 0.0192
680 - 690 nm	0.9544 ± 0.0041	0.9828 ± 0.0031	**1350 - 1360 nm**	0.3307 ± 0.0380	0.3403 ± 0.0389
690 - 700 nm	0.9658 ± 0.0033	0.9946 ± 0.0050	**1360 - 1370 nm**	0.0262 ± 0.0092	0.0269 ± 0.0094
700 - 710 nm	0.9763 ± 0.0032	1.0054 ± 0.0059	**1370 - 1380 nm**	0.2933 ± 0.0834	0.3017 ± 0.0856
710 - 720 nm	0.9662 ± 0.0031	0.9950 ± 0.0067	**1380 - 1390 nm**	0.1607 ± 0.0521	0.1653 ± 0.0535

720 – 730 nm	0.9840 ± 0.0038	1.0133 ± 0.0081	**1390 – 1400 nm**	0.2342 ± 0.0623	0.2409 ± 0.0639
730 – 740 nm	0.9823 ± 0.0040	1.0116 ± 0.0083	**1400 – 1410 nm**	0.3783 ± 0.0754	0.3892 ± 0.0773
740 – 750 nm	0.9742 ± 0.0041	1.0032 ± 0.0081	**1410 – 1420 nm**	0.7501 ± 0.0554	0.7722 ± 0.0561
750 – 760 nm	0.9977 ± 0.0046	1.0274 ± 0.0089	**1420 – 1430 nm**	0.9692 ± 0.0353	0.9980 ± 0.0341
760 – 770 nm	0.9190 ± 0.0058	0.9464 ± 0.0048	**1430 – 1440 nm**	0.9623 ± 0.0312	0.9909 ± 0.0292
770 – 780 nm	0.9964 ± 0.0044	1.0261 ± 0.0086	**1440 – 1450 nm**	1.1396 ± 0.0276	1.1735 ± 0.0247
780 – 790 nm	0.9894 ± 0.0045	1.0189 ± 0.0086	**1450 – 1460 nm**	1.0185 ± 0.0200	1.0488 ± 0.0164
790 – 800 nm	0.9801 ± 0.0049	1.0093 ± 0.0086	**1460 – 1470 nm**	1.0110 ± 0.0205	1.0410 ± 0.0170
800 – 810 nm	0.9871 ± 0.0043	1.0166 ± 0.0077	**1470 – 1480 nm**	0.9836 ± 0.0206	1.0129 ± 0.0173
810 – 820 nm	0.9962 ± 0.0047	1.0259 ± 0.0082	**1480 – 1490 nm**	0.9814 ± 0.0199	1.0106 ± 0.0162
820 – 830 nm	1.0149 ± 0.0052	1.0451 ± 0.0087	**1490 – 1500 nm**	0.9935 ± 0.0205	1.0231 ± 0.0167
830 – 840 nm	0.9920 ± 0.0057	1.0215 ± 0.0078	**1500 – 1510 nm**	0.9795 ± 0.0204	1.0086 ± 0.0167
840 – 850 nm	0.9828 ± 0.0063	1.0121 ± 0.0081	**1510 – 1520 nm**	0.9815 ± 0.0209	1.0107 ± 0.0171
850 – 860 nm	0.9876 ± 0.0056	1.0170 ± 0.0073	**1520 – 1530 nm**	0.9819 ± 0.0211	1.0111 ± 0.0173
860 – 870 nm	1.0006 ± 0.0071	1.0304 ± 0.0088	**1530 – 1540 nm**	0.9669 ± 0.0209	0.9957 ± 0.0172
870 – 880 nm	1.0043 ± 0.0076	1.0343 ± 0.0084	**1540 – 1550 nm**	0.9613 ± 0.0210	0.9899 ± 0.0174
880 – 890 nm	0.9887 ± 0.0092	1.0182 ± 0.0099	**1550 – 1560 nm**	0.9634 ± 0.0214	0.9921 ± 0.0177
890 – 900 nm	0.9860 ± 0.0112	1.0154 ± 0.0117	**1560 – 1570 nm**	0.9756 ± 0.0216	1.0047 ± 0.0179
900 – 910 nm	0.9896 ± 0.0127	1.0191 ± 0.0130	**1570 – 1580 nm**	0.9745 ± 0.0221	1.0035 ± 0.0184
910 – 920 nm	0.9806 ± 0.0127	1.0098 ± 0.0125	**1580 – 1590 nm**	0.9697 ± 0.0217	0.9985 ± 0.0181
920 – 930 nm	1.0015 ± 0.0099	1.0313 ± 0.0097	**1590 – 1600 nm**	0.9862 ± 0.0218	1.0155 ± 0.0181
930 – 940 nm	0.8905 ± 0.0123	0.9170 ± 0.0123	**1600 – 1610 nm**	0.9659 ± 0.0217	0.9946 ± 0.0180
940 – 950 nm	0.9915 ± 0.0107	1.0211 ± 0.0108	**1610 – 1620 nm**	0.9599 ± 0.0212	0.9885 ± 0.0177
950 – 960 nm	0.9489 ± 0.0073	0.9772 ± 0.0051	**1620 – 1630 nm**	0.9616 ± 0.0213	0.9902 ± 0.0177
960 – 970 nm	1.0081 ± 0.0063	1.0382 ± 0.0033	**1630 – 1640 nm**	0.9577 ± 0.0209	0.9862 ± 0.0174
970 – 980 nm	0.9869 ± 0.0061	1.0163 ± 0.0026	**1640 – 1650 nm**	0.9413 ± 0.0199	0.9693 ± 0.0167

4.5.2 JRC Spectrafy SolarSIM D2

Absolute Ratio R_{10}

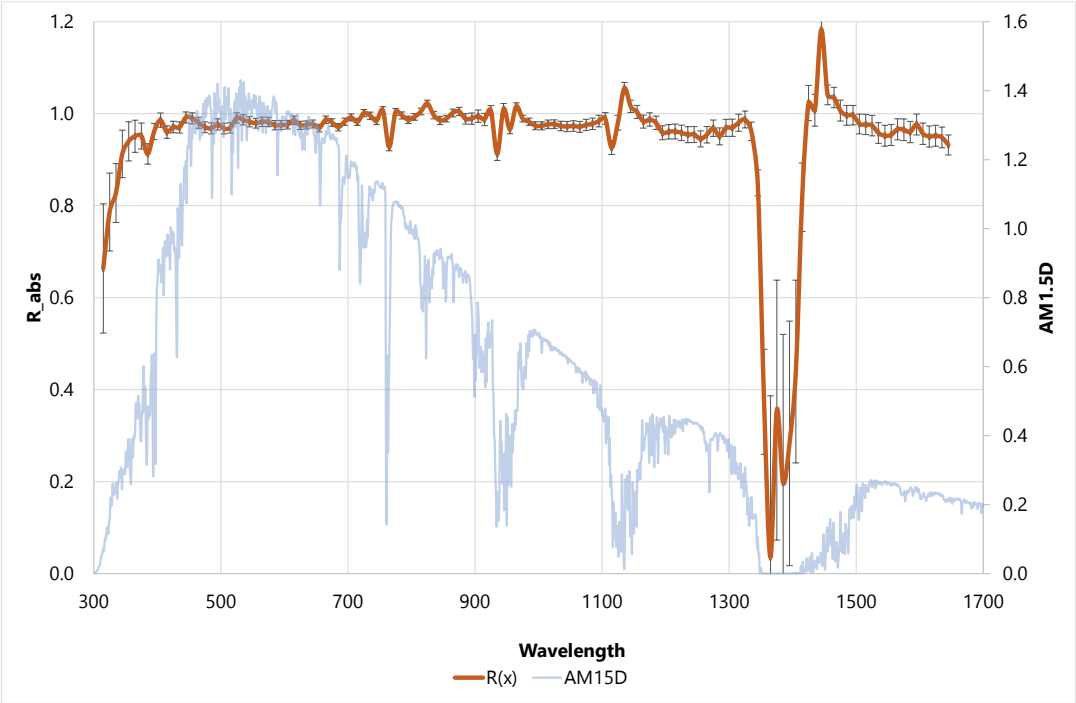

Relative Ratio R^*_{10}

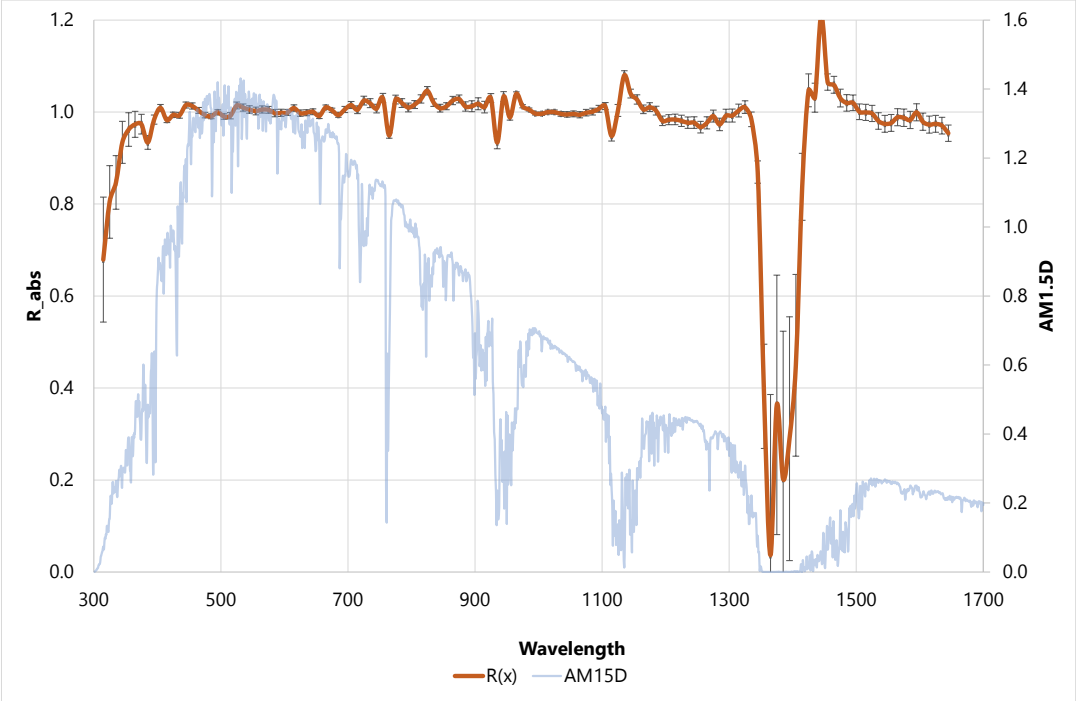

Figure 9: performance indicators of spectroradiometer Spectrafy Solar SIM D2 (JRC ESTI)

Table 13: tabulated values of performance indicaotrs for Spectrafy Solar SIM D2 (JRC ESTI)

λ	R10 absolute	R10 relative	λ	R10 absolute	R10 relative
310 - 320 nm	0.6637 ± 0.0932	0.6792 ± 0.0922	**980 - 990 nm**	0.9825 ± 0.0078	1.0056 ± 0.0033
320 - 330 nm	0.7862 ± 0.0665	0.8046 ± 0.0636	**990 - 1000 nm**	0.9739 ± 0.0082	0.9968 ± 0.0032
330 - 340 nm	0.8275 ± 0.0529	0.8469 ± 0.0493	**1000 - 1010 nm**	0.9736 ± 0.0086	0.9965 ± 0.0037
340 - 350 nm	0.9127 ± 0.0471	0.9341 ± 0.0426	**1010 - 1020 nm**	0.9770 ± 0.0091	0.9999 ± 0.0041
350 - 360 nm	0.9400 ± 0.0400	0.9620 ± 0.0350	**1020 - 1030 nm**	0.9770 ± 0.0094	1.0000 ± 0.0044
360 - 370 nm	0.9510 ± 0.0331	0.9733 ± 0.0276	**1030 - 1040 nm**	0.9732 ± 0.0100	0.9961 ± 0.0051
370 - 380 nm	0.9514 ± 0.0270	0.9737 ± 0.0209	**1040 - 1050 nm**	0.9720 ± 0.0108	0.9949 ± 0.0059
380 - 390 nm	0.9124 ± 0.0202	0.9339 ± 0.0140	**1050 - 1060 nm**	0.9732 ± 0.0111	0.9961 ± 0.0063
390 - 400 nm	0.9611 ± 0.0171	0.9837 ± 0.0098	**1060 - 1070 nm**	0.9714 ± 0.0115	0.9943 ± 0.0067
400 - 410 nm	0.9860 ± 0.0152	1.0092 ± 0.0073	**1070 - 1080 nm**	0.9756 ± 0.0119	0.9986 ± 0.0071
410 - 420 nm	0.9600 ± 0.0130	0.9826 ± 0.0055	**1080 - 1090 nm**	0.9780 ± 0.0122	1.0010 ± 0.0074
420 - 430 nm	0.9711 ± 0.0123	0.9939 ± 0.0056	**1090 - 1100 nm**	0.9839 ± 0.0123	1.0070 ± 0.0076
430 - 440 nm	0.9702 ± 0.0119	0.9930 ± 0.0063	**1100 - 1110 nm**	0.9898 ± 0.0125	1.0131 ± 0.0079
440 - 450 nm	0.9920 ± 0.0119	1.0153 ± 0.0067	**1110 - 1120 nm**	0.9263 ± 0.0139	0.9481 ± 0.0106
450 - 460 nm	0.9899 ± 0.0118	1.0132 ± 0.0069	**1120 - 1130 nm**	0.9804 ± 0.0155	1.0034 ± 0.0130
460 - 470 nm	0.9803 ± 0.0116	1.0034 ± 0.0066	**1130 - 1140 nm**	1.0553 ± 0.0136	1.0800 ± 0.0106
470 - 480 nm	0.9706 ± 0.0116	0.9934 ± 0.0060	**1140 - 1150 nm**	1.0161 ± 0.0134	1.0400 ± 0.0099
480 - 490 nm	0.9681 ± 0.0118	0.9909 ± 0.0054	**1150 - 1160 nm**	1.0037 ± 0.0142	1.0273 ± 0.0104
490 - 500 nm	0.9767 ± 0.0119	0.9997 ± 0.0054	**1160 - 1170 nm**	0.9828 ± 0.0139	1.0059 ± 0.0094
500 - 510 nm	0.9677 ± 0.0113	0.9904 ± 0.0058	**1170 - 1180 nm**	0.9874 ± 0.0142	1.0106 ± 0.0096
510 - 520 nm	0.9693 ± 0.0110	0.9920 ± 0.0069	**1180 - 1190 nm**	0.9800 ± 0.0143	1.0030 ± 0.0097
520 - 530 nm	0.9909 ± 0.0111	1.0142 ± 0.0076	**1190 - 1200 nm**	0.9585 ± 0.0145	0.9810 ± 0.0101
530 - 540 nm	0.9865 ± 0.0109	1.0097 ± 0.0078	**1200 - 1210 nm**	0.9608 ± 0.0150	0.9834 ± 0.0107
540 - 550 nm	0.9824 ± 0.0107	1.0055 ± 0.0082	**1210 - 1220 nm**	0.9613 ± 0.0157	0.9839 ± 0.0114
550 - 560 nm	0.9793 ± 0.0106	1.0023 ± 0.0084	**1220 - 1230 nm**	0.9583 ± 0.0162	0.9809 ± 0.0119
560 - 570 nm	0.9824 ± 0.0103	1.0055 ± 0.0078	**1230 - 1240 nm**	0.9544 ± 0.0166	0.9769 ± 0.0122
570 - 580 nm	0.9818 ± 0.0100	1.0049 ± 0.0074	**1240 - 1250 nm**	0.9546 ± 0.0167	0.9771 ± 0.0124
580 - 590 nm	0.9749 ± 0.0098	0.9978 ± 0.0081	**1250 - 1260 nm**	0.9451 ± 0.0165	0.9673 ± 0.0122
590 - 600 nm	0.9753 ± 0.0096	0.9983 ± 0.0077	**1260 - 1270 nm**	0.9541 ± 0.0171	0.9765 ± 0.0128
600 - 610 nm	0.9762 ± 0.0093	0.9991 ± 0.0065	**1270 - 1280 nm**	0.9686 ± 0.0173	0.9913 ± 0.0130
610 - 620 nm	0.9856 ± 0.0092	1.0088 ± 0.0069	**1280 - 1290 nm**	0.9508 ± 0.0174	0.9731 ± 0.0132
620 - 630 nm	0.9747 ± 0.0088	0.9976 ± 0.0068	**1290 - 1300 nm**	0.9693 ± 0.0181	0.9920 ± 0.0138
630 - 640 nm	0.9757 ± 0.0087	0.9986 ± 0.0065	**1300 - 1310 nm**	0.9696 ± 0.0182	0.9923 ± 0.0139
640 - 650 nm	0.9777 ± 0.0084	1.0007 ± 0.0064	**1310 - 1320 nm**	0.9804 ± 0.0182	1.0034 ± 0.0139
650 - 660 nm	0.9688 ± 0.0082	0.9916 ± 0.0058	**1320 - 1330 nm**	0.9874 ± 0.0181	1.0106 ± 0.0139
660 - 670 nm	0.9870 ± 0.0081	1.0102 ± 0.0050	**1330 - 1340 nm**	0.9616 ± 0.0192	0.9842 ± 0.0156
670 - 680 nm	0.9808 ± 0.0080	1.0039 ± 0.0045	**1340 - 1350 nm**	0.8497 ± 0.0238	0.8695 ± 0.0212
680 - 690 nm	0.9706 ± 0.0078	0.9935 ± 0.0048	**1350 - 1360 nm**	0.3736 ± 0.0426	0.3820 ± 0.0433
690 - 700 nm	0.9825 ± 0.0076	1.0056 ± 0.0069	**1360 - 1370 nm**	0.0356 ± 0.0125	0.0364 ± 0.0127
700 - 710 nm	0.9920 ± 0.0077	1.0153 ± 0.0078	**1370 - 1380 nm**	0.3555 ± 0.1005	0.3633 ± 0.1025
710 - 720 nm	0.9820 ± 0.0075	1.0051 ± 0.0085	**1380 - 1390 nm**	0.1976 ± 0.0637	0.2019 ± 0.0650

720 – 730 nm	1.0014 ± 0.0079	1.0249 ± 0.0098	**1390 – 1400 nm**	0.2834 ± 0.0753	0.2896 ± 0.0768
730 – 740 nm	0.9958 ± 0.0078	1.0192 ± 0.0099	**1400 – 1410 nm**	0.4395 ± 0.0873	0.4494 ± 0.0888
740 – 750 nm	0.9844 ± 0.0078	1.0075 ± 0.0095	**1410 – 1420 nm**	0.8185 ± 0.0610	0.8375 ± 0.0610
750 – 760 nm	1.0070 ± 0.0082	1.0307 ± 0.0102	**1420 – 1430 nm**	1.0233 ± 0.0390	1.0472 ± 0.0375
760 – 770 nm	0.9274 ± 0.0074	0.9492 ± 0.0056	**1430 – 1440 nm**	1.0076 ± 0.0347	1.0311 ± 0.0325
770 – 780 nm	1.0037 ± 0.0080	1.0273 ± 0.0098	**1440 – 1450 nm**	1.1825 ± 0.0309	1.2103 ± 0.0281
780 – 790 nm	0.9962 ± 0.0077	1.0196 ± 0.0096	**1450 – 1460 nm**	1.0408 ± 0.0223	1.0652 ± 0.0189
790 – 800 nm	0.9867 ± 0.0079	1.0099 ± 0.0096	**1460 – 1470 nm**	1.0351 ± 0.0229	1.0594 ± 0.0195
800 – 810 nm	0.9930 ± 0.0072	1.0164 ± 0.0087	**1470 – 1480 nm**	1.0068 ± 0.0228	1.0304 ± 0.0198
810 – 820 nm	1.0049 ± 0.0071	1.0285 ± 0.0092	**1480 – 1490 nm**	0.9964 ± 0.0216	1.0198 ± 0.0182
820 – 830 nm	1.0223 ± 0.0074	1.0464 ± 0.0095	**1490 – 1500 nm**	0.9967 ± 0.0212	1.0201 ± 0.0173
830 – 840 nm	0.9971 ± 0.0080	1.0206 ± 0.0085	**1500 – 1510 nm**	0.9778 ± 0.0211	1.0007 ± 0.0170
840 – 850 nm	0.9853 ± 0.0089	1.0085 ± 0.0085	**1510 – 1520 nm**	0.9764 ± 0.0215	0.9993 ± 0.0175
850 – 860 nm	0.9892 ± 0.0071	1.0125 ± 0.0077	**1520 – 1530 nm**	0.9741 ± 0.0217	0.9969 ± 0.0177
860 – 870 nm	1.0016 ± 0.0085	1.0252 ± 0.0092	**1530 – 1540 nm**	0.9580 ± 0.0215	0.9805 ± 0.0175
870 – 880 nm	1.0048 ± 0.0089	1.0284 ± 0.0088	**1540 – 1550 nm**	0.9521 ± 0.0216	0.9744 ± 0.0177
880 – 890 nm	0.9888 ± 0.0111	1.0121 ± 0.0101	**1550 – 1560 nm**	0.9539 ± 0.0219	0.9763 ± 0.0180
890 – 900 nm	0.9895 ± 0.0121	1.0128 ± 0.0120	**1560 – 1570 nm**	0.9660 ± 0.0222	0.9887 ± 0.0183
900 – 910 nm	0.9947 ± 0.0134	1.0181 ± 0.0133	**1570 – 1580 nm**	0.9650 ± 0.0227	0.9876 ± 0.0187
910 – 920 nm	0.9875 ± 0.0132	1.0107 ± 0.0129	**1580 – 1590 nm**	0.9601 ± 0.0223	0.9827 ± 0.0184
920 – 930 nm	1.0068 ± 0.0110	1.0305 ± 0.0100	**1590 – 1600 nm**	0.9765 ± 0.0224	0.9995 ± 0.0184
930 – 940 nm	0.9123 ± 0.0126	0.9337 ± 0.0125	**1600 – 1610 nm**	0.9564 ± 0.0222	0.9789 ± 0.0184
940 – 950 nm	1.0100 ± 0.0122	1.0338 ± 0.0110	**1610 – 1620 nm**	0.9504 ± 0.0217	0.9728 ± 0.0179
950 – 960 nm	0.9659 ± 0.0091	0.9885 ± 0.0061	**1620 – 1630 nm**	0.9520 ± 0.0218	0.9744 ± 0.0180
960 – 970 nm	1.0160 ± 0.0079	1.0398 ± 0.0045	**1630 – 1640 nm**	0.9483 ± 0.0214	0.9706 ± 0.0176
970 – 980 nm	0.9894 ± 0.0072	1.0126 ± 0.0037	**1640 – 1650 nm**	0.9321 ± 0.0202	0.9540 ± 0.0168

5 Absolute Cavity Radiometers

The ISRC hosted ten Absolute Cavity Radiometers (ACR), listed in the table below.

Table 14: Absolute Cavity Radiometers participating at the ISRC 2023

Cavity	Owner	Traceability
PMO6 81109	JRC ESTI	Davos IPC-XIII (2021)(**)
PMO6 911204	JRC ESTI	Davos IPC-XIII (2021) (**)
TMI 68835	JRC ESTI	Davos IPC-XIII (2021) (**)
PMO8 F191-P02	Davos Instruments	---
PMO8 F201-007A	PMOD/WRC(*)	Davos IPC-XIII (2021) (**)
PMO6 0401	PMOD/WRC(*)	Davos IPC-XIII (2021) (**)
PMO8 F211-001	CIEMAT	Davos IPC-XIII (2021) (**)
PMO6 1609	CIEMAT	Davos IPC-XIII (2021) (**)
AHF 0000	W. Zaaiman	Davos IPC-XIII (2021) (**)
TMI 67604	W. Zaaiman	Davos IPC-XIII (2021) (**)

(*) Instrument owned by Davos PMOD/WRC but operated by Davos Instruments at the ISRC

(**) Participating in the calculation of the assigned value for the comparison

Due to issues related to logistics and transport, two cavities arrived at the Observatory only on day three (28 June), and therefore their result refers to one day of measurements. Another cavity did not measure on the first day. All the other cavities submitted data for three consecutive days (26-28 June) but after the filtering process the second day was discarded due to too few valid points.

The time frames with clear sky conditions used for the restricted ACR comparison is the same resulting from the filtering process described in [3.3]. Therefore the sky stability filtering has been done using the JRC sensors.

Regarding the reference assigned value, it has been agreed by the participants that for the restricted Intercomparison of the cavity radiometers, at any instant of time it is the average of the 9 radiometers with a valid WRR factor from the latest IPC-XIII held in Davos in 2021.

Each participant was allowed to submit data in his preferred file format, therefore also for the data sets of the cavities a preliminary time syncing has been performed to align all the time series.

The parameters used to assess the performance of each instrument at any instant of time t is then given by the ratio

$$R_p(t) = \frac{G_p(t)}{\hat{G}(t)} \qquad \text{(Eq. 4)}$$

being $G_p(t)$ the measured irradiance value of participant p at time t, and $\hat{G}(t)$ the assigned value at the same time. A graphical representation of the statistical highlights and distribution of the ratios is shown in Fig. 5.1 for the two days with a sufficient number of valid points.

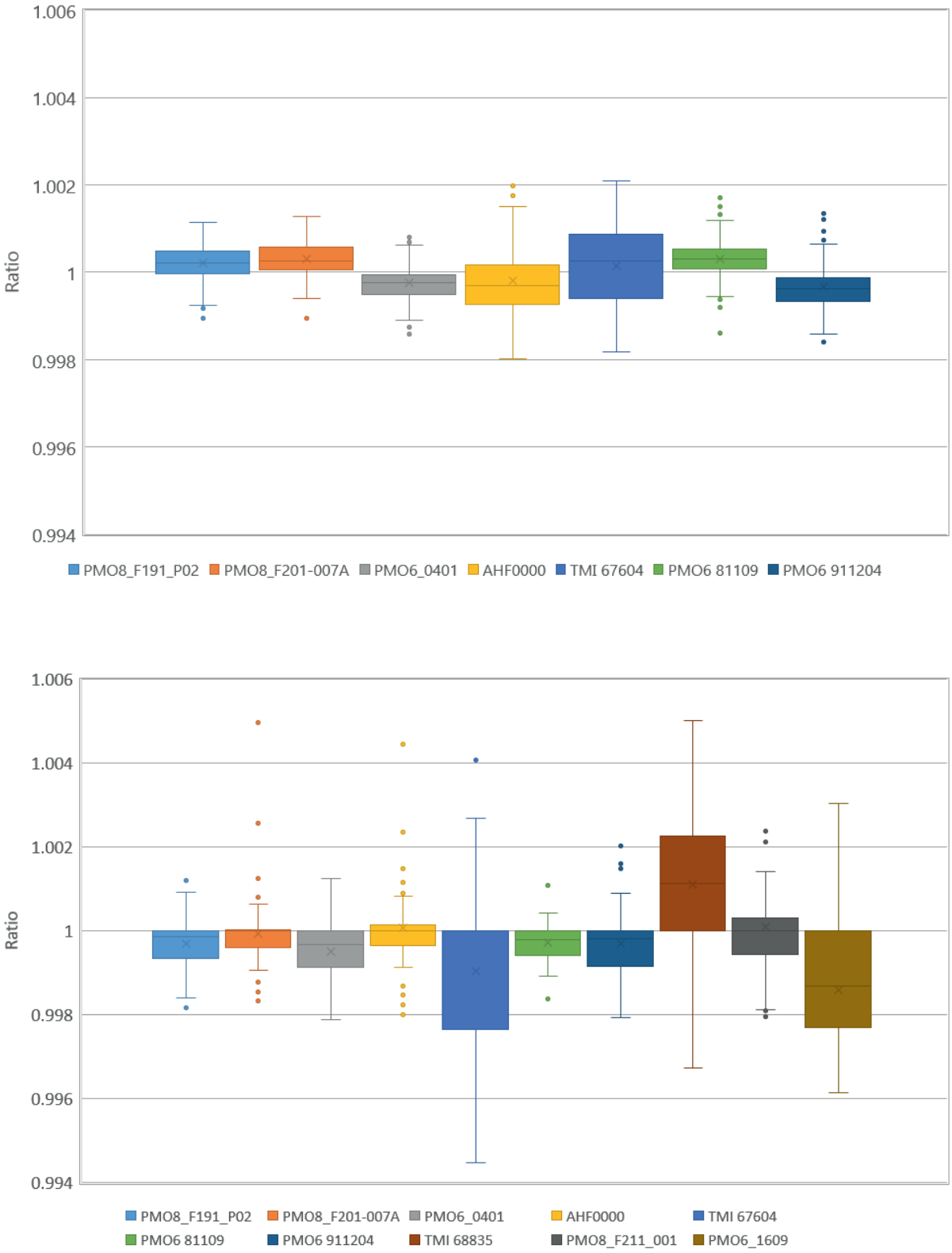

Figure 10: distribution of Rp (t) divided by instrument for two different days: 26 June (top) and 28 June (bottom)

HOW TO READ A "BOX AND WHISKER" PLOT

A so-called "box and whisker" plot is a useful way of graphically representing the data distribution around an average value. It shows data divided into quartiles, evidencing the mean and the outliers. The mean is represented by the cross "X" inside the box; the vertical amplitude of the box is such as to contain the points within the two central quartiles of the statistical distribution of the entire data set. Each box has two vertical lines (the whiskers) to put in evidence the distribution of points in the upper and lower quartiles. Any point outside the whiskers might be considered as an outlier.

The numerical results of each instrument is shown in Table 15. For each day R is the ratio calculated with (Eq. 4).

Table 15: Statistical overview of the Intercomparison restricted to the absolute cavity radiometers

	26-Jun			28-Jun		
	R	2σ	$2\sigma_{rel}$	R	2σ	$2\sigma_{rel}$
PMO8_F191_P02	1.00022	0.00081	0.08%	0.99969	0.00120	0.12%
PMO8_F201-007A	1.00030	0.00077	0.08%	0.99992	0.00177	0.18%
PMO6_0401	0.99975	0.00074	0.07%	0.99951	0.00141	0.14%
AHF0000	0.99981	0.00152	0.15%	1.00006	0.00184	0.18%
TMI 67604	1.00015	0.00191	0.19%	0.99903	0.00410	0.41%
PMO6 81109	1.00031	0.00087	0.09%	0.99971	0.00091	0.09%
PMO6 911204	0.99967	0.00109	0.11%	0.99969	0.00149	0.15%
TMI 68835				1.00111	0.00334	0.33%
PMO8_F211_001				1.00010	0.00451	0.45%
PMO6_1609				0.99859	0.00325	0.33%

The restricted intercomparison amongst the Absolute Cavity Radiometers was done in order to assess the metrological stability of the nine instruments having a WRR factor assigned at the last IPC-XIII held in Davos (CH) in 2021. Given that the next IPC-XIV is planned for 2025, following the typical 5-years cycle, an intermediate metrological exercise in between is of fundamental importance for the reliability of results.

Given the deviations shown above, all the nine radiometers have proven to be stable respect to their latest WRR factors.

6 Part 4: Custom sensors and prototypes

6.1 ARBOL

ARBOL (Array of BOLometers) is a sun photometer developed over the last few years by the Instrumental Optics Laboratory at the Physics Department - University of Milan. It has been developed within the GAIA project, funded by the by the European Social Fund through the Autonomous Region of Aosta Valley.

General layout

The instrument is composed by six telescopes, designed to collect sunlight or skylight at the AERONET wavelengths, and one for solar tracking through an active feedback. All components are built with anticorodal aluminium alloy to limit the total weight.

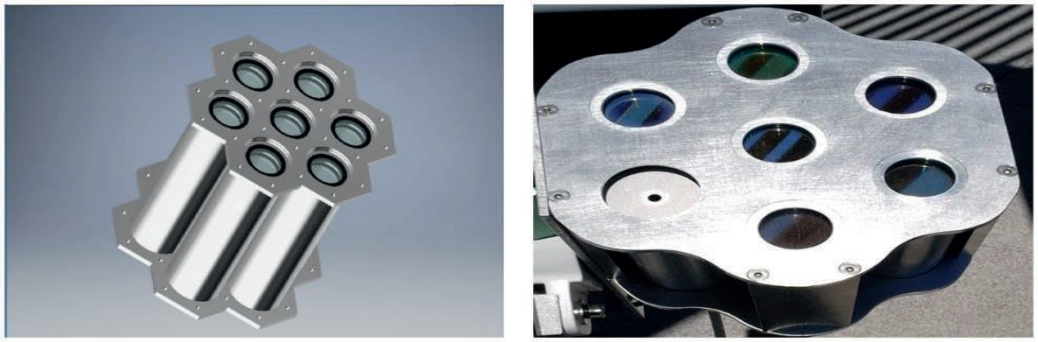

Figure 11: On the left, ARBOL mechanical rendering; on the right, a picture of the instrument. Each telescope is 130mm long (0.1mm tolerance) and the internal and external diameters are 35mm and 38 mm respectively

ARBOL telescopes and optical components

The six telescopes measure six different wavelengths through specific narrow-bandpass filters. Fig. 7 describes the longitudinal section of a telescope.

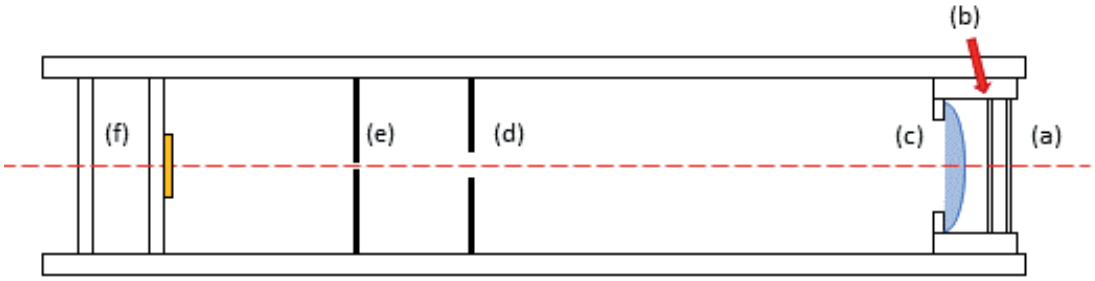

Figure 12: Internal layout of ARBOL telescopes. From right to left: (a)borosilicate optical window; (b) bandpass filter; (c) objective plano-convex lens; (d) baffle; (e) pinhole; (f) PCB

The incoming light (from right to left) firstly passes through a plane parallel optical window (a) composed by borosilicate glass which protects all the subsequent optical components from dust. Next, a bandpass filter (b) with a FWHM of about 10 nm operates the spectral selection at the desired wavelengths: 400 nm, 500 nm, 675 nm, 870 nm, 940 nm, and 1020 nm. The filter selection is a trade-off between the need of adopting the Lambert-Beer law for monochromatic light and to keep the measured power high enough. A FWHM = 10 nm is an ideal compromise.

A plano-convex lens (c) of borosilicate glass collects light in its focal plane and a pinhole (e), centred on the lens focal spot, fixes the instrument field of view (specifically, ARBOL's field of view is FOV=1.1°); a baffle (d), centred in the aluminium disk, reduces the stray light between (c) and (e). At the detection plane two PCBs (f) mounting the photodiode and front-end electronicsare installed.

ARBOL is equipped with two different sensors. The photodiode Hamamatsu S5107 is used for 500 nm, 675 nm and 870 nm spectral channels; the photodiode Hamamatsu S1337 is used for 400 nm, 940 nm and 1020 nm. Both are silicon photodiodes and their spectral response ranges from 320/340 nm up to 1100 nm, with a sensitivity peak at 960 nm). Nevertheless, there are some differences in the spectral response curve and, more importantly, in the temperature coefficient curve (Fig. 8): the larger the coefficient, more the photosensitivity is affected by temperature variations.

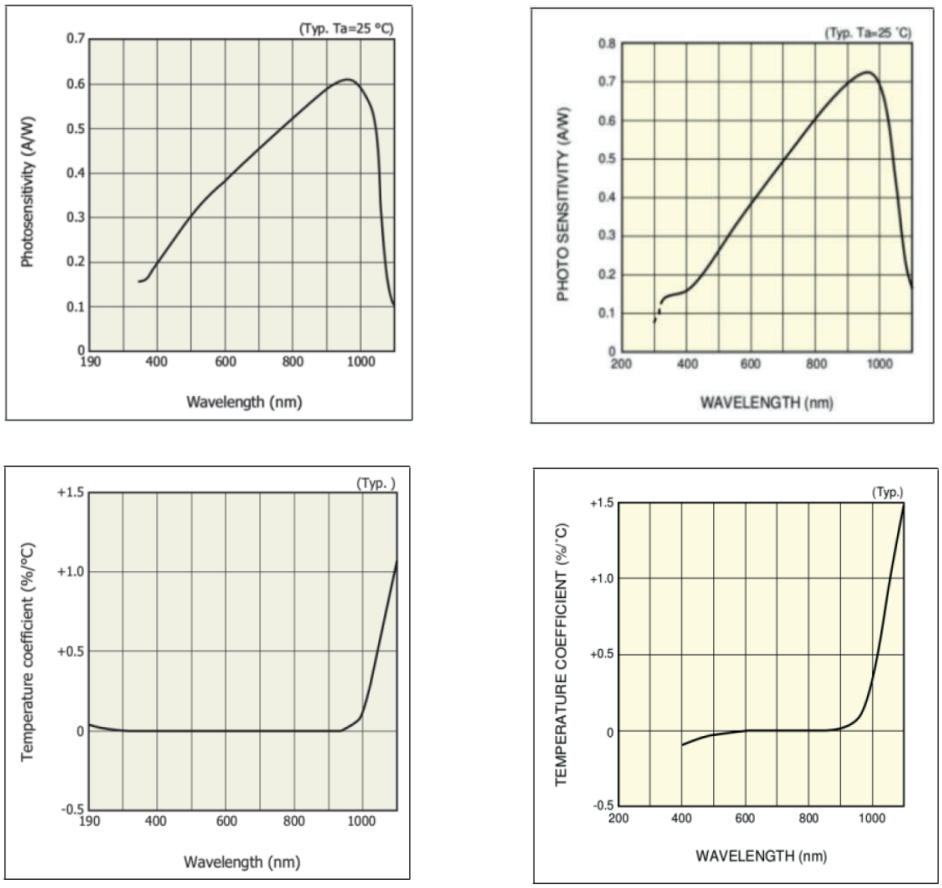

Figure 13: Comparison between S1337 (on the left) and S5107 (on the right) spectral response, at the standard temperature T=25°C, and photosensitivity thermal coefficient.

Tracking system

ARBOL is fixed on a commercial tracking mount (EQ3 from Sky-Watcher) composed of a tripod and a mechanical body that can rotate along two orthogonal axes driven by two stepper motors. We operate the EQ3 in altazimuthal configuration, in order to allow the use of only one motor to span the entire almucantar line. The whole tracking system is controlled by a Raspberry Pi3.

The tracking telescope is simpler than the other six: it only consists of a diaphragm and four-quadrant silicon photodiode (QPD) mounted on a PCB, appropriately separated. The QPD centre precisely intersects the telescope axis and. The QPD signals are sent a 16-bits ADC (model ADS1115) connected to the Raspberry Pi3. A python software controls the tracking feedback. The

position and precise timing are retrieved through a GNSS module and sent from the Raspberry Pi3, where an open source software (pysolar) provides the Sun coordinates to the mount. The system checks differences in height and azimuth each second. This feedback system has proven to be able to track the Sun from sunrise down to sunset.

6.2 RSE CPV-PV Hybrid module Functional Unit

The CPV concentration photovoltaic technology is based on high efficiency multijunction solar cells, that allow, for the same surface area, generating higher power peaks than flat plate photovoltaic systems. However, so far, the building integration of solar concentrators has been hindered by the need to install the CPV modules on high-precision bi-axial solar trackers, that guarantee the continuous alignment between the photovoltaic cells and optics. Therefore, the solar tracker has represented a bottleneck for the diffusion of CPV technology in terms of reliability, costs, weight, and dimensions. To overcome this limit, RSE has started developing a solar tracking system, designed to be integrated within the CPV photovoltaic module, whose actuators are based on Shape Memory Alloy (SMA), which can reduce the electro-mechanical complexity of the tracker with a consequent reduction of environmental impact and costs. While SMA actuator are not new in the solar energy community, RSE has developed an original control system that allows precisely controlling the SMA actuators for the CPV application.

A second limitation of CPV technology is its capacity to convert only the direct and not the diffuse solar irradiance component. For this reason, RSE has also addressed its research in the development of hybrid CPV/PV modules consisting of both high-efficiency CPV cells (installed on a planar moving frame actuated by the innovative solar tracking system previously described) and low-cost conventional photovoltaic cells capable of converting the diffused light.

In collaboration with an engineering Italian company, RSE has already developed a first functional unit which includes the CPV cells, and the integrated solar tracking system based on SMA actuators (see Figure 9) useful to test the SMA tracker concept.

On the movable frame, four CPV cells have been installed (with an area equal to 9 mm2) able to convert the direct sunlight, focused by four lenses (which can be pointed out by looking at the front side of the unit). Furthermore, several PV cells are included on the front side of the unit with the purpose to power in the future the internal tracking.

The measurement campaign carried out during the International Spectroradiometer and Broadband Radiometer Intercomparison 2022 was useful to demonstrate the correct functioning of the solar tracking system integrated in the unit, even under strong daily temperature variation, that could potentially have a negative impact on the accuracy of the SMA actuators control. The current-voltage curves of the active part of the functional unit (CPV array only) were also acquired in order to preliminary assess the power performance.

Figure 14: Front view of a functional unit of hybrid CPV / PV module with integrated solar tracking system based on SMA actuators, consisting of 4 lenses that focus the light on 4 high-efficiency CPV cells positioned on a moving frame that moves parallel to the p

7 Conclusions

The International Spectroradiometer and Broadband Radiometer Intercomparison (ISRC) took place in Lignan (AO) from 26th to 30th June 2022, hosted by the Astronomical Observatory of the Aosta Valley (OAVDA).

The 11th edition saw the participation of the European Space Agency, National Metrological Institutes, laboratories, universities, private companies and research organizations operating in different fields, mainly in the renewable energies sector, meteorology and climatology.

During the measurement campaign several spectroradiometers of different types were compared against the ESTI reference instruments to provide an assessment of their performance in different spectral bands of interest for many applications, ranging from studies on new materials for photovoltaics and their characterisation, space missions, development of measurement systems for collection of data for climatology models.

The broadband irradiance instruments of different participants have been compared against the ESTI set of Absolute Radiometric Cavities and the reference pyranometer in order to give information about their conversion factors.

For the first time, the presence of ten Absolute Cavity Radiometers (of which nine directly traceable to WRR via IPC-XIII) allowed to perform a restricted Intercomparison amongst ACRs. In this case the assigned value has been agreed to be the arithmetic average of the nine cavities traceable to IPC.

The ISRC is an annual event organised by the Joint Research Centre of the European Commission, in particular by the ESTI laboratories based at the Ispra site in Italy, and having no participation fees for the participants. It is a free useful service to support research bodies and small/medium enterprises operating in the solar energy sectors, and a high level metrology assessment for top class institutes.

The intercomparison between the absolute cavity radiometers confirmed the stability of all the instruments respect to their WRR factors assigned at the latest IPC-XIII in Davos (2021), as an intermediate verification in view of the next IPC-XIV planned for 2025. Even considering the limited number of data points, all of them were within ±0.02% respect to the calculated assigned values.

The performance of spectroradiometers is absolute terms suggests that improvements in the calibration procedures are needed for some participants, due to the absolute deviations respect to the reference spectra (R_{10} performance indicator). In relative terms (R_{10}*), the agreement is much better and thus the impact on the calculation of the spectral mismatch factor for PV devices is limited.

References

[1]. Galleano, R., Zaaiman, W., Morabito, P., Minuto, A., Spena, A., Bartocci, S., Fucci, R., Leanza, G., Pavanello, D., Virtuani, A., Fasanaro, D., Catena, M., & Norton, M. (2012). Intercomparison of spectroradiometers for solar spectral irradiance measurements. Preliminary results. AIP Conference Proceedings, 1477. https://doi.org/10.1063/1.4753853

[2]. Webpage of the European Solar test Installation: https://joint-research-centre.ec.europa.eu/european-solar-test-installation_en

[3]. Pavanello, D., Galleano, R., Zaaiman, W., Ankit, M., Kouremeti, N., Gröbner, J., Hoogendijk, K., Po, M., Lisbona, E. F., Alius, W., Dosenicova, D., Kroeger, I., Friedrich, D., Haverkamp, E., Minuto, A., Celi, E., Pravettoni, M., Bellenda, G., & Fucci, R. (2020). Results of the IX International Spectroradiometer Intercomparison and impact on precise measurements of new photovoltaic technologies. Progress in Photovoltaics: Research and Applications. https://doi.org/10.1002/pip.3347

[4]. Galleano, R., Zaaiman, W., Morabito, P., Minuto, A., Spena, A., Bartocci, S., Fucci, R., Leanza, G., Pavanello, D., Virtuani, A., Fasanaro, D., Catena, M., & Norton, M. (2012). Intercomparison of spectroradiometers for solar spectral irradiance measurements. Preliminary results. AIP Conference Proceedings, 1477. https://doi.org/10.1063/1.4753853

[5]. Galleano, R., Zaaiman, W., Virtuani, A., Pavanello, D., Morabito, P., Minuto, A., Spena, A., Bartocci, S., Fucci, R., Leanza, G., Fasanaro, D., & Catena, M. (2014). Intercomparison campaign of spectroradiometers for a correct estimation of solar spectral irradiance: Results and potential impact on photovoltaic devices calibration. Progress in Photovoltaics: Research and Applications, 22(11). https://doi.org/10.1002/pip.2361

[6]. Galleano, R., Zaaiman, W., Strati, C., Bartocci, S., Pravettoni, M., Marzoli, M., Fucci, R., Leanza, G., Timo, G., Minuto, A., Catena, M., Aleo, F., Takagi, S., Akiyama, A., Nunez, R., & Belluardo, G. (2015). Second international spectroradiometer intercomparison: results and impact on PV device calibration. Progress in Photovoltaics: Research and Applications, 23, 929–938. https://doi.org/10.1002/pip.2511

[7]. Galleano, R., Zaaiman, W., Alonso-Alvarez, D., Minuto, A., Ferretti, N., Fucci, R., Marzoli, M., Manni, L., Halwachs, M., Friederick, M., Plag, F., Friedrich, D., & Haverkamp, E. (2016). Preliminary Results of the Fifth International Spectroradiometer Comparison for Improved Solar. Eu Pvsec, 1465–1469. https://www.researchgate.net/publication/304658276

[8]. Forgan, B. W. (1996). A new method for calibrating reference and field pyranometers. Journal of Atmospheric and Oceanic Technology, 13(3), 638–645. https://doi.org/10.1175/1520-0426(1996)013<0638:ANMFCR>2.0.CO;2

[9]. International Standard ISO 9059:1990. ISO IEC, 13.

[10]. International Standard ISO 9847:2023 ed.2. ISO IEC.

[11]. Website of the Astronomical Observatory of the Aosta Valley: https://www.oavda.it/

[12]. International Standard ISO 9846:1993

List of abbreviations and definitions

JRC Joint Research Centre

ISRC International Spectroradiometer Intercomparison

ESTI European Solar Test Installation

PV Photovoltaics

ISO International Organisation for Standardisation

DNI Direct Normal Irradiance

GNI Global Normal Irradiance

λ Wavelength

AO Aosta (Province of Italy)

OAVDA Osservatorio Astronomico della Valle d'Aosta

ACR Absolute Cavity Radiometer

$R_{10}(\lambda_1,\lambda_2)$ Performance indicator expressing the agreement of the absolute spectral content in the band (λ_1,λ_2)

$R_{10}^*(\lambda_1,\lambda_2)$ Performance indicator expressing the agreement of the relative spectral content in the band (λ_1,λ_2)

List of tables

List of figures

GETTING IN TOUCH WITH THE EU

In person

All over the European Union there are hundreds of Europe Direct centres. You can find the address of the centre nearest you online (european-union.europa.eu/contact-eu/meet-us_en).

On the phone or in writing

Europe Direct is a service that answers your questions about the European Union. You can contact this service:

— by freephone: 00 800 6 7 8 9 10 11 (certain operators may charge for these calls),

— at the following standard number: +32 22999696,

— via the following form: european-union.europa.eu/contact-eu/write-us_en.

FINDING INFORMATION ABOUT THE EU

Online

Information about the European Union in all the official languages of the EU is available on the Europa website (european-union.europa.eu).

EU publications

You can view or order EU publications at op.europa.eu/en/publications. Multiple copies of free publications can be obtained by contacting Europe Direct or your local documentation centre (european-union.europa.eu/contact-eu/meet-us_en).

EU law and related documents

For access to legal information from the EU, including all EU law since 1951 in all the official language versions, go to EUR-Lex (eur-lex.europa.eu).

Open data from the EU

The portal data.europa.eu provides access to open datasets from the EU institutions, bodies and agencies. These can be downloaded and reused for free, for both commercial and non-commercial purposes. The portal also provides access to a wealth of datasets from European countries.

Science for policy

The Joint Research Centre (JRC) provides independent, evidence-based knowledge and science, supporting EU policies to positively impact society

EU Science Hub
joint-research-centre.ec.europa.eu

@EU_ScienceHub

EU Science Hub - Joint Research Centre

EU Science, Research and Innovation

EU Science Hub

@eu_science